Arokiasamy, P, Abdullah, MMAB, Abd Rahim, SZ, Sadique, M, Ming, LY, Mohd Salleh, MAA, Mohd Arif Zainol, MRR and Ghazali, CMR

Diverse material based geopolymer towards heavy metals removal: A review

JOURNAL OF MATERIALS RESEARCH AND TECHNOLOGY 2023;22:126–156

Available online at www.sciencedirect.com

jmr&t Journal of Materials Research and Technology

journal homepage: www.elsevier.com/locate/jmrt

Review Article

Diverse material based geopolymer towards heavy metals removal: a review

Pilomeena Arokiasamy [a,b], *Mohd Mustafa Al Bakri Abdullah* [a,b,*], *Shayfull Zamree Abd Rahim* [a,c], *Monower Sadique* [d], *Liew Yun Ming* [a,b], *Mohd Arif Anuar Mohd Salleh* [a,b], *Mohd Remy Rozainy Mohd Arif Zainol* [e], *Che Mohd Ruzaidi Ghazali* [f]

[a] *Centre of Excellence Geopolymer & Green Technology (CEGeoGTech), Universiti Malaysia Perlis (UniMAP), 01000 Perlis, Malaysia*
[b] *Faculty of Chemical Engineering & Technology, Universiti Malaysia Perlis (UniMAP), 01000 Perlis, Malaysia*
[c] *Faculty of Mechanical Engineering & Technology, Universiti Malaysia Perlis (UniMAP), 01000 Perlis, Malaysia*
[d] *School of Civil Engineering and Built Environment, Liverpool John Moores University, United Kingdom*
[e] *River Engineering and Urban Drainage Research Centre (REDAC), Universiti Sains Malaysia, 14300 Penang, Malaysia*
[f] *Universiti Malaysia Terengganu, Faculty of Ocean Engineering Technology and Informatics, 21030 Terengganu, Malaysia*

ARTICLE INFO

Article history:
Received 28 June 2022
Accepted 15 November 2022
Available online 19 November 2022

Keywords:
Heavy metals
Adsorption
Alkaline activation
Geopolymer
Adsorbent

ABSTRACT

Metakaolin is a commonly used aluminosilicate material for the synthesis of geopolymer based adsorbent. However, it presents characteristics that restrict its uses such as weak rheological properties brought on by the plate-like structure, processing challenges, high water demand and quick hydration reaction. Industrial waste, on the other hand, contains a variety of components and is a potential source of aluminosilicate material. Geopolymer adsorbent synthesized by utilizing industrial waste contains a wide range of elements that offer better ion-exchangeability and increase active sites on the surface of geopolymer. However, limited studies focused on the synthesized of geopolymer based adsorbent by utilizing industrial waste for heavy metal adsorption in wastewater treatment. Therefore, this paper reviews on the raw materials used in the synthesis of geopolymer for wastewater treatment. This would help in the development of low cost geopolymer based adsorbent that has a great potential for heavy metal adsorption, which could deliver double benefit in both waste management and wastewater treatment.

* Corresponding author.
E-mail address: mustafa_albakri@unimap.edu.my (M.M.A.B. Abdullah).
https://doi.org/10.1016/j.jmrt.2022.11.100

1. Introduction

The rapid industrialization and urbanization in recent decades affect the quality and quantity of water supplies. Particularly, the uncontrolled discharge of untreated industrial wastewater causing serious environmental damages including heavy metal pollution. Heavy metal ion refer to the metallic element that has atomic weight in the range between 63.5 g/mol and 200.6 g/mol and specific gravity of more than 5.0 g/cm^3 [1–4]. According to the United States Environmental Protection Agency (US EPA), the most toxic heavy metal includes arsenic (As), copper (Cu), mercury (Hg), nickel (Ni), cadmium (Cd), lead (Pb) and chromium (Cr) [5,6]. Industrial processes like metal plating, fertilizer manufacture, petrochemical, paper making, and mining operations have significantly increased the mobilization of the heavy metals [3]. A serious threat is posed to plant, animal, and human life due to the non-biodegradable, bioaccumulation and toxicity properties of heavy metals even at low concentration [4,7–9]. Serious hazard such as cancers, cardiovascular, brain tumor, nerve damage problems are brought on by heavy metal ions after entering into human bodies. Therefore, decontamination of heavy metals from aqueous solution is crucial to protect public health and the environment.

A number of techniques have been available to remove heavy metal ions from wastewater prior to being released into the environment. Elimination of heavy metals can be achieved through various methods including membrane filtration, ion exchange, chemical precipitation, electrocoagulation and adsorption [1,3,10,11]. Sludge generation, maintenance, equipment cost, energy consumption, low efficiency, and time consuming methods are all disadvantages of most of the techniques mentioned [10,12,13]. By contrast, adsorption is regarded as the most effective physicochemical technique for heavy metal removal because of its ease of handling, low capital cost, high efficiency, and suitability for both batch and continuous processes [1,14,15]. The examples of adsorbents are activated carbon (AC), biochar (BC), clay mineral, chitosan, lignin, and geopolymer [16–18].

Among various type of adsorbents, geopolymer has gained great interest among researchers due to its excellent immobilization effect. Geopolymer is an inorganic polymer with a three-dimensional (3D) polymeric structure and pores formed by the condensation of aluminosilicate mineral powder being added into an alkali solution at temperatures below 100 °C, which was invented by Joseph Davidovits in 1970 [19–21]. Similar zeolite structure of geopolymer provides excellent adsorbent properties, which can aid in heavy metal removal from wastewater. Geopolymer has similar properties to zeolite and has a high capacity for cation exchange and a strong affinity for cationic heavy metals with the presence of Al in the geopolymer matrix [19,22,23]. In addition, geopolymer can be synthesized by using geological origin such as kaolin, metakaolin and dolomite and industrial waste such as slag, fly ash (FA) and sludge as an aluminosilicate precursor.

Metakaolin (MK) is a commonly used aluminosilicate material for the synthesis of geopolymer based adsorbent as it offers unique adsorption properties such as different structural selectivity, optimal sorption capacity and cation exchangeability for various metal cations, which can be used to optimize the process design of wastewater treatment [24]. However, it presents characteristics that restrict its uses such as weak rheological properties brought on by the plate-like structure, processing challenges, increased cost, high water demand, quick hydration reactions, and high heat gain in the

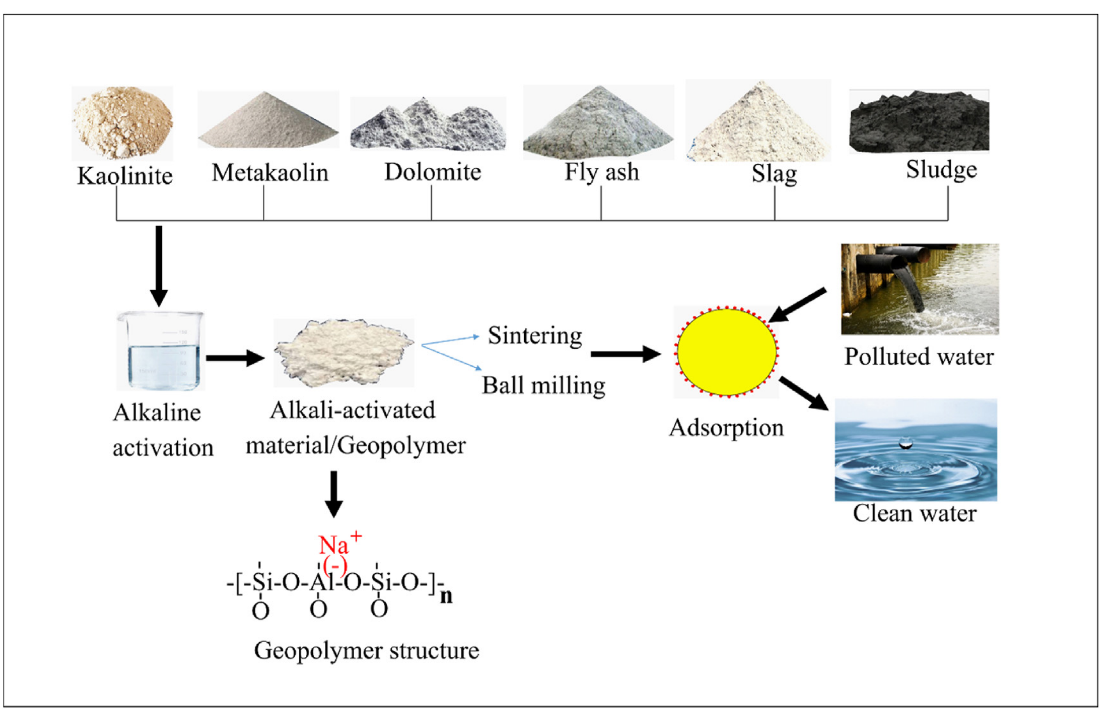

Fig. 1 – Graphical illustration of geopolymer synthesis for heavy metal adsorption.

Table 1 – Toxic heavy metals in industrial wastewater [10].

Heavy metals	Manufacturing industries	Toxicity to human health	Maximum contaminant level (mg/L)
Cu	Electrical, plating, rayon	Gastrointestinal, liver or kidney damage	0.25000
Ni	Electroplating, steel	Dermatitis, nausea, chronic asthma, coughing, human carcinogen	0.20000
Hg	Chlor-alkali, chemical, scientific instruments	Causes damage to nervous system, kidney and vision	0.00003
As	Phosphate fertilizer, metal hardening, paints and textile	Causes damage to skin, eyes and liver	0.05000
Cd	Electroplating, phosphate fertilizer, pigments	Kidney damage, carcinogenic	0.01000
Pb	Battery, paints	Kidney problems and diminished neuronal development	0.00600
Cr	Metal plating, tanning, rubber, photographic	Allergic, dermatitis, diarrhea, nausea and vomiting	0.05000

initial phases [25]. On the other hand, MK as an industrial waste is a potential aluminosilicate material as it contained a wide range of components contributed to improved adsorption efficiency of geopolymer adsorbent depending on the processing and raw material properties [26,27]. The presence of metal oxide and inorganic salts in the industrial waste increased the active sites on the surface of geopolymer and offer combined contribution of cation exchange, ion precipitation and ion complexation with heavy metal [27–29]. However, limited number of studies focused synthesized of industrial waste based geopolymer adsorbent for heavy metal adsorption in the wastewater treatment. Thus, this paper reviews the diverse material used for serving wastewater treatment as illustrated in Fig. 1. Additionally, this paper reviews the mechanisms involved in the heavy metal adsorption and also studies the important parameters such as concentration of alkaline activator, alkaline activator ratio, solid-to-liquid ratio and curing temperature on the geopolymerization process. Besides, the environmental approaches to modify the physical properties of geopolymer adsorbents is also provided in this work. Hence, this review would guide in clean production of cost-effective adsorbent, which could provide double benefit in waste management and wastewater treatment.

2. Heavy metal ion

Heavy metal ions have been extensively exploited and used in various fields due to their excellent physicochemical and diverse electronic properties, resulting in large number of heavy metal ions being discharged into air, water and soil causing serious environmental issues [30–32]. Toxic heavy metals in industrial wastewater are as tabulated in Table 1. Heavy metal ions can be categorized into essential ions and non-essential ions. Essential ions such as cobalt (Co), Cr, Ni, zinc (Zn), iron (Fe) and manganese (Mn) are also known as trace elements and are required by the organism and micronutrient to stabilize the molecules through electrostatic interactions, and are involved in redox processes, used as catalysts in enzymatic reactions, and also in maintaining the osmotic balance [33,34]. On the other hand, non-essential ions such as Cd, Hg and Pb have no biological responses and are harmful to the organism even at very low concentration [10,35,36]. As aforementioned, according to the US EPA, the most toxic heavy metal includes As, Cu, Hg, Ni, Cd, Pb and Cr [5,6,37]. These ions do not disintegrate naturally due to the inorganic structure, and are thus stable in the environment, posing a risk of accumulating as hazardous and carcinogenic substances in living organisms through the food cycle [38,39]. Therefore, these heavy metal ions need to be removed from the wastewater prior to being disposed into the ecosystem. There are several existing methods for removing heavy metals from wastewater that have been used in the past.

The existing methods for heavy metal removal include membrane separation, electrocoagulation, adsorption, chemical precipitation, biological treatment and ion exchange [10–12,40,41]. Some techniques are extremely effective at removing heavy metal ions, but these techniques do not appear to be feasible in industrial applications due to the high cost, high energy consumption, sludge generation, chemical usage and low removal rate [11,12,42]. One of the most cost-effective methods is adsorption, which has been reported to be an effective method for heavy metal removal from wastewater based on certain specific criteria such as cost, operation, chemical used and sludge generation [10,11,40,42]. There are two forms of adsorption: physisorption and chemisorption based on the type of bonding between the adsorbent and the adsorbate.

3. Types of adsorptions

The nature of the interactions between the adsorbate and the adsorbent determines how adsorption and desorption processes are classified, which can be categorized into two types: chemical adsorption and physical adsorption which are also known as chemisorption and physisorption respectively [42–46]. These two mechanisms can be distinguished in terms of specificity, bonding, enthalpy, surface area, molecular layer, and temperature of the process. Chemisorption is the attraction between the adsorbate and adsorbent caused by the chemical reactions occurring between the adsorbate and the adsorbent, which create covalent or ionic bonds such as the adsorption of oxygen and hydrogen with metals to form metal oxides hydride [44,47,48]. The types of adsorption forces and desorption capability of an adsorbent are determined by chemical structures, primarily functional groups [44,49,50]. While, physisorption can be determined when the relatively weak electrostatic interactions are the main interaction

Table 2 – Comparison between chemisorption and physisorption.

Aspects	Chemisorption	Physisorption
Nature	Irreversible	Reversible
Adsorption layer	Monolayer	Multilayer
Temperature	High temperature	Low temperature
Specificity	Specific	Non-specific
Force of attraction	Specific forces (Ionic or covalent chemical bond)	Universal weak forces (van der Waals force)
Enthalpy	High enthalpy (80–240 kJ/mol)	Low enthalpy (20–40 kJ/mol)
Activation energy	Needs high value	Not needed
Example	Ionic interactions	Van der Waals interactions
		Hydrophobicity
		Hydrogen bonding
		π-π interactions

between the adsorbate and adsorbent and the accessibility of an adsorbent for heavy metals is determined by physical structures, specifically surface area and pore size [49,51–53]. The comparisons between chemisorption and physisorption are tabulated in Table 2.

Chemical and physical structures of adsorbents will aid in the adsorption process by influencing the adsorbate–adsorbent interaction. The removal efficiency and adsorption capacity of heavy metal ions from aqueous solution by prepared adsorbents will be evaluated by conducting adsorption test either in batch system or fixed-bed columns [54,55]. Various materials, such as zeolite, activated carbon, resin, chitosan, and others, have been discovered and used for water remediation for decades [16,17,56,57] with activated carbon being the benchmark for adsorbent material due to its unique adsorption capacity [17,58]. However, due to the high cost of carbon material, low cost geopolymer adsorbent has attracted the researcher's interest in water treatment application as it is composed of zeolite like structure and expected to have unique adsorption properties as well as zeolite [58,59].

4. Geopolymer

Geopolymers are a class of inorganic materials and amorphous 3D aluminosilicate binder materials that can be produced in the temperature range of 20–100 °C through alkaline activation of aluminosilicates [54,60–62]. Geopolymerization enables the production of low-cost, low dense, porous ceramic-like inorganic self-supporting membranes and filters with the absence of sintering [63,64]. The polymeric bonds of geopolymers are composed of polysialates (Si–O–Al). The sialate network structure contains tetrahedral $[SiO4]^{4-}$and $[AlO4]^{5+}$, sharing oxygen atoms [65,66]. During the reaction, Al undergoes changes from an octahedral (VI) to a tetrahedral (IV) coordination. Thus, in order to neutralize the negative charge of the tetravalent (Al), cations of Na^+, K^+, Li^+, Ca^{2+} must be present in the voids of the polysialate [65,66]. Therefore, the following empirical formula was proposed for polysialates:

$$Mn[(-SiO_2)z - AlO_2]n.w\ H_2O \tag{1a}$$

Whereby M is alkali cation, n is the degree of polycondensation, and z is the Si/Al ratio on the basic silico-aluminate unit of the polysialate.

Moreover, geopolymer is widely used in construction industry and also in innovative applications such as biomaterials, catalysis, pH buffering and filtering [67–69]. A 3D and tetrahedral structure of Si–O–Al, with negatively charged sites is capable of attracting positively charged solutes [59,70,71]. In addition, geopolymer should have similar properties to zeolite with to the presence of polymeric Si–O–Al framework in geopolymer, which is comparable to that found in zeolites. However, the main difference between the geopolymers structure and zeolites is that it is amorphous at ambient temperature [72]. Apart from that, geopolymer has a significant amount of mesoporosity with sizes ranging from 10 to 50 nm and can restrict the mobility of heavy metal ions when entering into the framework [73,74]. Additionally, the surface properties of adsorbents have a significant impact on the adsorption rate and capacity [75]. Geopolymers are well known materials which often consist of high pore volume and large surface area [75]. FA-based geopolymer adsorbent with surface area and pore volume of 56.0 m^2/g and 0.14 cm^3/g was produced by solid fusion of FA at 550 °C for the removal of methylene blue (MB) and crystal violet (CR) dyes [68]. Besides, the porous geopolymer spheres made from slag and designed to remove Pb^{2+} have a surface area of 100.99 m^2/g. Other than that, geopolymers are made up of cyclic molecular chains composed of a “crystal-like” structure. Closed cage-like cavity generated by the conjunction of ring molecules can aid in the removal of heavy metals or other pollutants by fixing it in the cavity [22,76,77].

In addition, the main ingredients used to produce geopolymers are aluminosilicate source and alkaline activator, such as sodium hydroxide (NaOH), potassium hydroxide (KOH), sodium silicate (Na_2SiO_3), and potassium silicate (K_2SiO_3) [78,79]. The starting ingredients for the synthesis of geopolymers can be synthetic, natural aluminosilicate minerals, or industrial aluminosilicate wastes such as slags, waste glass, FA, or rice husk ash. The raw materials and the activator media are typically blended for 10–15 min before being put into a mold. The geopolymer pastes are then cured at a temperature between 20 and 100 °C [20,80]. The resulting material is washed with distilled water, until the washing water has a neutral pH, and then treated at a temperature below 100 °C in order to prevent the precipitation of hydroxides. The produced geopolymer is then grounded and sieved to a specific size to be used as an adsorbent material. Furthermore, during the geopolymerization process, the mechanisms such as

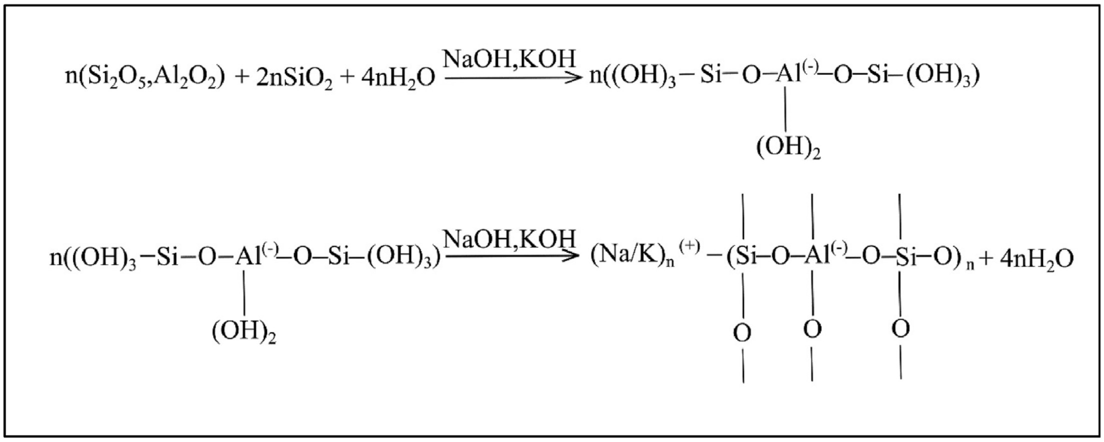

Fig. 2 – Schematic representations of geopolymer [83].

dissolution, gelation, and condensation reactions occur simultaneously to produce geopolymer materials [81,82]. First of all, the aluminosilicate parent mineral is broken down through alkaline digestion and hydrolysis processes and the formation of aluminate and silicate monomers is aided by the dissolution [83] as expressed in Fig. 2. Then, the Al^{3+} and Si^{4+} species are transferred into geopolymer material condense to form a gel with relatively large networks. Finally, the growing gel causes polycondensation processes that result in the development of an aluminosilicate network [83].

Besides, geopolymers have a quick setting time with a high resulting strength, excellent thermal and chemical resistance, high thermal shock resistance, and low permeability. Other than that, due to its low manufacturing temperature, lower energy consumption and low CO_2 emissions, geopolymer materials are considered environmentally benign [84–87]. Geopolymers have remarkable advantages such as low cost, facile synthesis and local availability of raw materials [22,88]. The geopolymer production technique in an aqueous media allows for custom-tailored porosity. It tends to have a porous and open microstructure, especially when it has high alkali content and low calcium content [89,90]. However, brittleness, efflorescence, and excessive drying shrinkage of the hardened geopolymer are limitations of the geopolymer [91]. The high alkali content in the pore solution, as well as the weak binding of Na^+ in the geopolymer structure, caused an increase in the Na mobility in the pore solution, resulting in severe geopolymer efflorescence [89,92]. The advantages and disadvantages of the synthesized geopolymer are tabulated in Table 3.

Geopolymers have been utilized successfully for the adsorption of heavy metal ions such as Cd^{2+}, Ni^{2+}, Pb^{2+}, Cu^{2+}, and Ni^{2+}, boron, fluoride, phosphate and radionuclide and dyes such as MB, congo red, methyl violet and methyl orange from wastewater [82,99,100]. Recently, Li et al. [101] used synthesized electrolytic Mn residue-based geopolymer adsorbent to immobilize Pb^{2+} and Cd^{2+}. Besides, Zhang et al. [102] utilized Pb, Zn slag-based geopolymer to immobilize Pb^{2+} and Zn^{2+}. The non-bridging oxygen bonds and bridging oxygen bonds that are present in the Si sources include Si–O–OH, Si–O–Na, OH–Si–O–Al–OH and Si–O–Si, while bonds that are present in Al sources are Al–OH and OH–Si–O–Al–OH. Si–OH, Al–OH, and OH–Si–O–Al–OH are some of the ligands that can be employed to activate the functional adsorption groups by coordinating with heavy metals [103]. Meanwhile, the ion exchange mechanism between heavy metal ions and Na^+ units in Si–O–Na is another possible interaction [103]. The Si–O–Si unit does not have an adsorption function, but it serves as the adsorbent's skeleton and strengthens the geopolymer adsorbent. However, the mechanisms involved in the adsorption process of heavy metals by geopolymer adsorbents still not yet fully understood.

4.1. *Adsorption mechanism on geopolymer based adsorbent*

Immobilization of heavy metals by geopolymer can be classified into two categories. The first type is heavy metal-containing waste mixed with geopolymer precursors to prevent heavy metals from leaching from the waste. The second type involves mixing geopolymer precursors with highly water soluble heavy metal salts to investigate the interaction between heavy metal ions and the geopolymer framework [86,87,94]. The preparation of highly soluble form of heavy metal salt or real wastewater is required to conduct the adsorption experiment for the second type. Previous

Table 3 – Advantages and disadvantages of synthesized geopolymer.

Advantages	Disadvantages
• Low cost and a wide range of resources [22,93]	• Excess alkali metal [89,92]
• Simple and feasible [90,94]	• Efflorescence [89,92]
• Tunable properties [89,90]	• Degradation of geopolymer [89,92]
• Low carbon footprint [85,95]	• Brittleness [91,96]
• Reduction in greenhouse emission [84,85]	• Shrinkage after rapid drying [64,91]
• Less energy consumption [97,98]	
• Low permeability [45]	
• Resistance to acid attack [45]	
• Cage-like structure [23,76]	

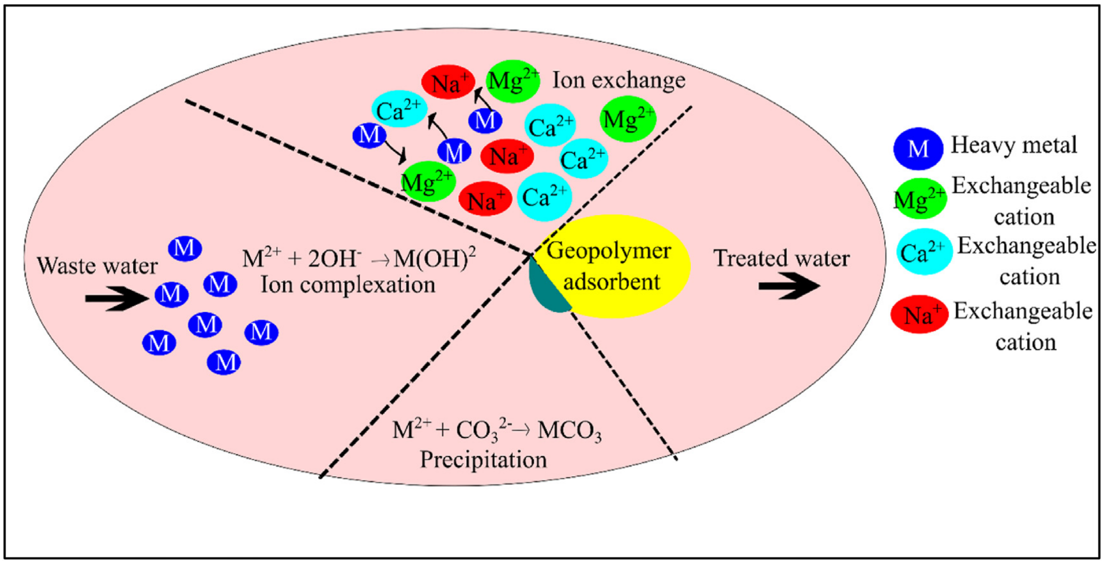

Fig. 3 – Different adsorption mechanism [110].

researchers claimed that geopolymers are effective in the removal of heavy metals and other pollutants such as harmful organic and inorganic leachates/effluents from industry and landfills through ion exchange between the solution and the adsorbent, surface complexation, or surface precipitation of low solubility chemicals [87,94,103,104].

Ion exchange is a removal technique in which an ion entrapped on the adsorbent surface is replaced by a similarly charged metal ion in a solution to maintain the electroneutrality between solid and solution [28,105]. A study by Blackford et al. [106] found that heavy metals are replaced with Na^+ in the geopolymer to maintain the charge balance of the geopolymer by observing the increment in the Na^+ leaching. In addition, Van Jaarsveld and Van Deventer et al. [107] claimed that Pb^{2+} might exchange with Na^+ due to its larger ionic radius (0.119 nm) than Na^+ (0.102 nm). Ion exchange interaction is not a single mechanism, while other removal mechanisms, such as surface complexation and surface precipitation occur together with this adsorption process as shown in Fig. 3 [105]. In chemisorption, surface complexation involves chemical interaction between heavy metal with the functional groups on the adsorbent surface [28,105,108]. The displacements in the peak of Fourier transform infrared spectroscopy (FTIR) and X-ray photoelectron spectroscopy (XPS) spectra indicate that functional groups are involved in the formation of complexes. In addition, surface precipitation is another process that has been widely reported [28,105,108]. The presence of soluble mineral components on the adsorbent surface permits the heavy metal ions to form insoluble metal oxides and hydroxides, resulting in surface precipitation. On the other hand, according to Long et al. [109], the environment for geopolymer polymerization contains a variety of Si and O elements that can react with Pb to produce Pb_3SiO_5.

Table 4 presents the summary of adsorption mechanism on geopolymer adsorbent. In 2019, Yan et al. [97] investigated the adsorption performance of heavy metal ions by geopolymer incorporated gangue microspheres. Based on FTIR results, after the integration of the gangue microsphere, the adsorbents' surfaces were characterized by rich functional groups, which facilitated the removal of heavy metal ions from wastewater as expressed in Fig. 4. Even after adsorption, this adsorbent retains a large number of functional hydroxyl groups such as–OH, –SiOH, and –AlOH which aid in the chemical bonding between adsorbent and heavy metal ions. Heavy metal ions that are positively charged at pH in the range 2–6 resulted in repulsion forces and electrostatic attraction forces between functional groups of the adsorbents and heavy metal ions. Besides, the optimization of porous structure by the addition of gangue microspheres enhances the adsorption performance of adsorbents. Nevertheless, Yan et al. [97] study failed to discuss on the effect of different gangue microsphere contents in the synthesis of geopolymer and also in the adsorption performance of heavy metals.

Moreover, Yu et al. [111] developed a mesoporous geopolymer from MK as an aluminosilicate material and cetyltrimethylammonium bromide (CTAB) as an organic modifier for the adsorption process of Cu^{2+} and Cr^{6+} from aqueous solution. In a binary system, the removal efficiency and adsorption capacity of modified geopolymer for Cr^{6+} are higher than in a single system. The adsorption of Cu^{2+} in the binary system was reduced slightly by the actions interfering ions, which encouraged the adsorption of Cr^{6+} by the formation of electrostatic shield against the electrostatic repulsion forces between Cr^{6+} cations as shown in Fig. 5. This is because, when Cr^{6+} aggregates around the adsorption site, it attracts Cu^{2+} in the solution to maintain electric neutrality. In addition, for certain concentrations of K^+ or Na^+ solution, the adsorbed geopolymers will undergo ion exchange again at which K^+ exchange Cu^{2+} and the initially adsorbed ions will be desorbed. Thus, energy dispersive X-ray spectroscopy (EDX) analysis should be conducted in this study to identify the compositional elements in the adsorbed geopolymer.

Table 4 – Adsorption mechanism of geopolymer adsorbent.

Author	Heavy metal ions	Source materials	Mechanisms	Findings
Yan et al. [97]	• Cu^{2+} • Cd^{2+} • Zn^{2+} • Pb^{2+}	• Coal gangue microspheres	• Physical • Chemical • Electrostatic • Ion exchange	• Porous structure of geopolymer was improved by the addition of gangue microspheres • Pb^{2+} has the highest adsorption capacity compared to other metal ions
Yu et al. [111]	• Cu^{2+} • Cr^{6+}	• MK • CTAB	• Electrostatic shield • Ion exchange	• Addition of CTAB improves geopolymer properties • Decrease in surface area with the addition of CTAB due to the attachment of CTA^{+}
Niu et al. [28]	• Cs^{+} • Sr^{2+} • Co^{2+}	• MK	• Ion exchange • Surface complexation • Precipitation	• K^{+} leaching was unaffected by the type of MK used • Cs^{+} removal never changed the surface charge of geopolymer whereas Sr^{2+} and Co^{2+} does
Yan et al. [104]	• Pb^{2+} • Ni^{2+}	• Carbon nanotube • FA • Slag	• Ion exchange • Electrostatic interaction • Hydrolysis • Flocculation • Complexation	• CNT addition affected the microstructure, surface area and pore volume of the geopolymer • The removal efficiency of Pb^{2+} was greater than Ni^{2+}
Ma et al. [112]	• Pb^{2+} • Ni^{2+}	• Foundry dust	• Coordination • Ion exchange • Electrostatic attractions	• Addition of H_2O_2 provides more adsorption sites for heavy metal ions • Adsorption capacity of Ni^{2+} by geopolymer hinder by Pb^{2+}
Su et al. [103]	• Cd^{2+}	• Slag • Macromolecular dithiocarbamate	• Inter-particle diffusion • Coordination • Chelation	• Dynamic adsorption has high adsorption capacity than static • Grafting of MDTC significantly improved structural properties with no phase changes

Similarly, Niu et al. [28] examined the adsorption behavior of radionuclide cations (Cs^{+}, Sr^{2+} and Co^{2+}) and anions (I^{-}, IO^{3-}, $SeO_3{}^{2-}$ and $SeO_4{}^{2-}$) by two types of MK-based geopolymer. During the adsorption process of Cs^{+}, the main mechanism involved in the removal process was one-to-one ion exchange mechanism between K^{+} and Cs^{+}. Whereas, one-to-one or one-to-two ion exchange and surface complexation mechanisms such as $SrOH^{+}$ and $CoOH^{+}$ were involved in the adsorption process of Sr^{2+} with additional precipitation mechanisms such as formation of cobalt blue ($CoAl_2O_4$) in Co^{2+}. Sr^{2+} binding can be thought of as pure ion exchange at low concentration at which one mole of Sr^{2+} adsorption releases two moles of K^{+}. On the other hand, at higher concentration of Sr^{2+}, more ions are entrapped due to one-to-one ion exchange and surface complexation. The leaching of Al from the geopolymer structure is required for the creation of cobalt blue, which could affect matrix stability. However, geopolymer lacks the capacity to directly absorb anions and thus further studies are required for the development of geopolymer on anions adsorption efficiency.

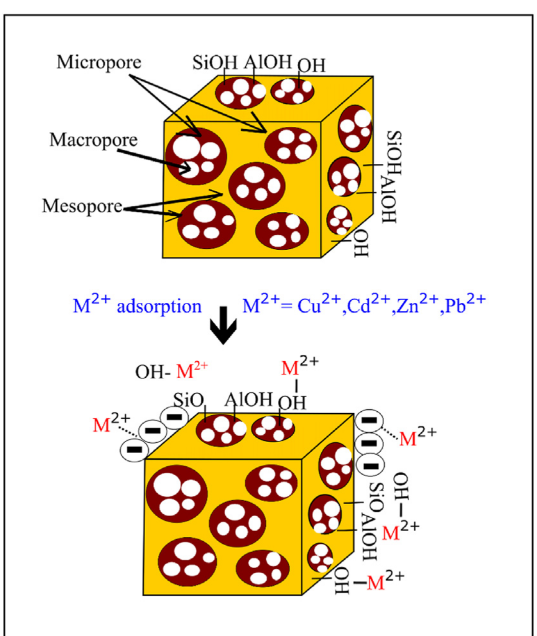

Fig. 4 – Adsorption mechanism of heavy metal in gangue microspheres based geopolymer.

Other than that, Yan et al. [104] evaluated the influence of carbon nanotube (CNT) on the phase formation, porous structure and adsorption mechanism of Pb^{2+}, Ni^{2+} and MB using spherical porous CNT-based geopolymer by employing FA and MK as the aluminosilicate materials. Upon geopolymerization, the geopolymer showed amorphous peak, which indicated that FA and MK may react with the activated solution while addition of CNT had no impact on the geopolymerization process of the geopolymer matrix. CNT did not participate in the geopolymerization reaction while the enhancement in the surface area and porous structure through the addition of CNT had aided in the physical adsorption mechanism. The adsorption process is further

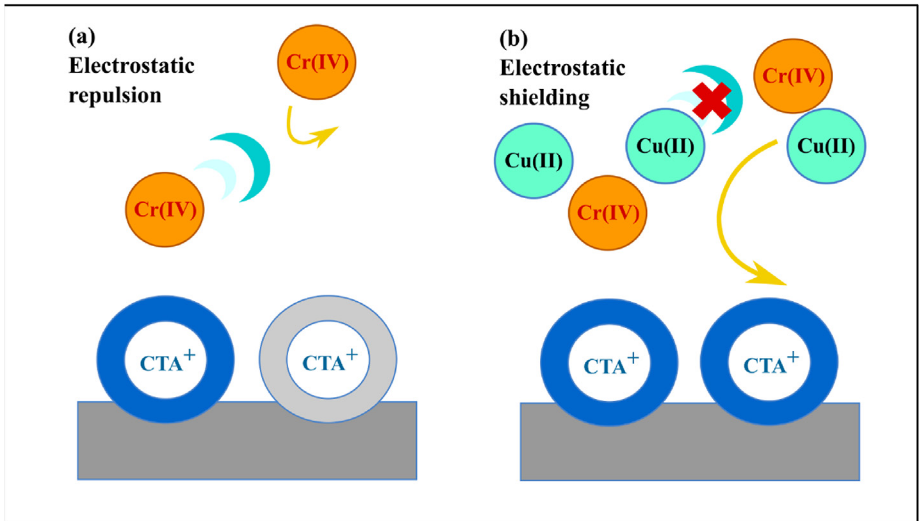

Fig. 5 – Shielding effect on the repulsion force between Cr^{6+} [111].

influenced by the cation exchange between cations in the solution and K^+ and Ca^{2+} in the geopolymer structure. The high adsorption capacity of the geopolymer spheres was also aided by the protonation and deprotonation of SiOH and AlOH groups. Specifically, Pb^{2+} has a substantially larger adsorption capacity than Ni^{2+}, owing to differences in hydrated ion size, free energy of hydration, and comparable atomic radii. However, in Yan et al. [104] study, the difference in the hydrated ion size, free energy of hydration and atomic radii between Pb^{2+} and Ni^{2+} were not discussed in detail.

In contrast, Ma et al. [112] synthesized porous foundry dust based geopolymer with and without the addition of hydrogen peroxide (H_2O_2) to observe the adsorption capacity of Pb^{2+} and Ni^{2+} from aqueous solution. The adsorption capacity of both metal ions by synthesized geopolymer with the addition of H_2O_2 was greater than without H_2O_2. In addition, the negative charge on the surface of geopolymer due to presence of significant amount of $[Al(OH)_4]^-$, $[SiO(OH)_3]^-$ and $[SiO_2(OH)_2]^{2-}$ was responsible for the electrostatic attraction between geopolymer and metal ions. Furthermore, after adsorption, the displacement of peaks corresponds to 1027 cm^{-1} to higher wavenumber and 458 cm^{-1} to lower wavenumber indicates the coordination reaction of Si–O–Al functional group with metal ions which changes the surface charge. Besides, a drop in the Na content at time after adsorption demonstrates the ion exchange mechanism between Na^+ of geopolymer and Pb^{2+} and Ni^{2+}. Nevertheless, it will be more understandable if this study could provide a schematic diagram, which can illustrate the mechanisms occurring during the adsorption of Pb^{2+} and Ni^{2+}.

In comparison, Su et al. [103] produced slag based geopolymer microsphere composite by grafting macromolecular dithiocarbamate (MDTC) in it to investigate the removal efficiency of Cd^{2+}. The Cd^{2+} concentration on the external surface of geopolymer composite was greater than inside of the geopolymer composite, demonstrating the involvement of the inter-particle diffusion process during adsorption. After adsorption by geopolymer composite, the peak at 1465 cm^{-1} which corresponds to N-CS_2 was displaced at 1418 cm^{-1} indicating formation of strong heavy metal–ligand bond between geopolymer and Cd^{2+}. Prior to MDTC grafting, the adsorption capacity of geopolymer depends on Si and Al hydroxyls present in the geopolymer. After grafting of MDTC, the Si–O–Si unit which acts as a skeleton of the adsorbent and does not exhibit adsorption effect was converted into active functional groups for adsorption as illustrated in Fig. 6. The grafting of MDTC could activate the Si–O–Si unit present in geopolymer by connecting the elements in between geopolymer and MDTC. However, the ion exchange mechanism between Si–O–Na unit and Cd^{2+} during the adsorption process was not clearly discussed by Su et al. [103].

The wastewater can be easily treated using geopolymer as a purifier with appropriate usage of precursors and synthetic techniques. Many materials that are rich in silicon (Si) and aluminum (Al) can be used in order to synthesize geopolymer. Based on the previous studies, geopolymer can be synthesized using raw materials which have high amount of Si and Al compounds such as MK, FA, slag, silica fume (SF), rice husk ash (RHA) and red mud (RD) [22,54,88,93,113]. Extending raw material resources for geopolymer synthesis and conducting additional research on its application in heavy metal pollution treatment are important for energy savings, waste reduction, resource recovery, and environmental protection [114–116].

4.2. *Raw materials for geopolymer synthesis*

Synthesis of geopolymer involves several steps such as preparation of alkaline solution, mixing of aluminosilicate sources with alkaline activator and curing process of prepared geopolymer paste as illustrated in Fig. 7 [60,117]. Therefore, the hardened paste will be crushed and sieved into the required particle size. Dissolution of Si and Al from the aluminosilicate sources, diffusion, reorientation of precursor ions, polymerization and condensation are the mechanisms involved in alkaline activation process [55,64,117,118]. The formation of geopolymer structures such as polysialate (PS), poly (sialate-siloxo) (PSS) and poly (sialate-disiloxo) (PSDS) based on the Si/Al ratio of the geopolymer matrix are formed depending on the SiO_2 to Al_2O_3 ratio of the raw material [55,119] as shown in

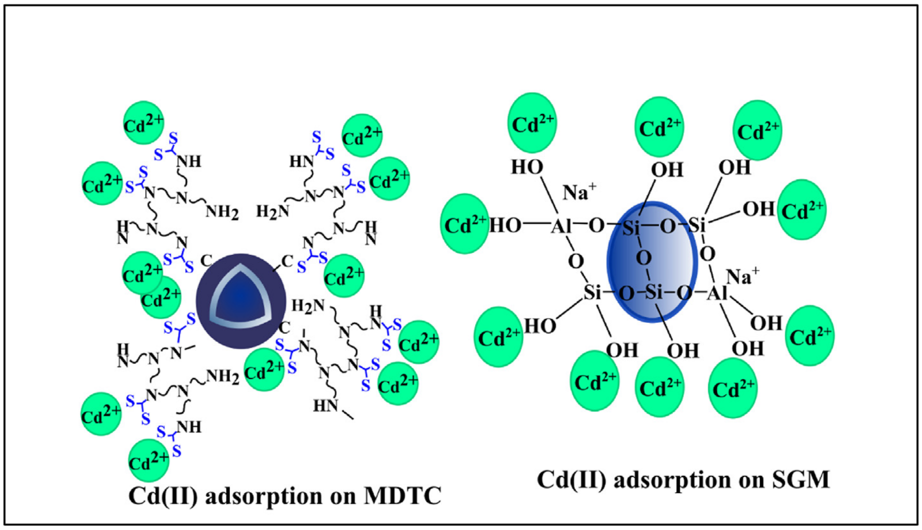

Fig. 6 – Adsorption mechanism on MD-Geopolymer composite [103].

Fig. 8. Si/Al ratio is a key consideration when choosing the right application for geopolymers. Si/Al adjustment is crucial to balance the mechanical strength and thermal behavior of geopolymer. This is because, when Si/Al = 1,2 and 3, it will form ceramic-like properties, adsorbent material and thermal protection material respectively [65,120,121]. Thus, the choice of appropriate precursor is crucial for efficient geo-polymerization process as the mole ratio of Si to Al is an essential parameter in the synthesis of geopolymer.

Kaolinite is the most common mineral in the kaolin group, which also includes dickite, nacrite, and halloysite [124,125]. Kaolin has low reactivity in alkali activation due this structural make up [126,127]. On the other hand, MK is a type of synthetic pozzolanic material which has high reactivity than kaolinite and has high purity than other clays [128,129]. Generally, MK is mainly composed of 50–55% SiO_2 and 40–45% Al_2O_3 [130,131]. MK, is made using heat treatment of kaolin [$Al_2Si_2(OH)_4$], one of naturally occurring clay minerals in the earth's crust, to temperatures between 600 and 850 °C. This is an endothermic reaction at which significant amount of energy is required to remove chemically bonded hydroxyl (OH^-). This heat treatment degrades the kaolin structure by removing the bonded OH^-, resulting in a disordered structure [93,132]. Dehydroxylation of kaolinite results in structural transition of highly reactivity MK from a pseudo-hexagonal or octahedral to a tetrahedral shape. MK is frequently used in the alkali activation process [76,128,133]. MK based geopolymers offers unique adsorption properties such as different structural selectivity, optimal sorption capacity and cation exchangeability for various metal cations which can be used to optimize the process design of wastewater treatment [24]. Other than that, MK based geopolymer has the ability to adsorb heavy metal ions through ion exchange mechanism and it also offers various kinds of binding sites for adsorption [89,113]. Nevertheless, layered structure of MK limits particles mobility during mixing and this make the reaction system of less workable [134]. Thus, MK based geopolymer necessitates low S/L ratio to obtain a homogenous reaction mixture.

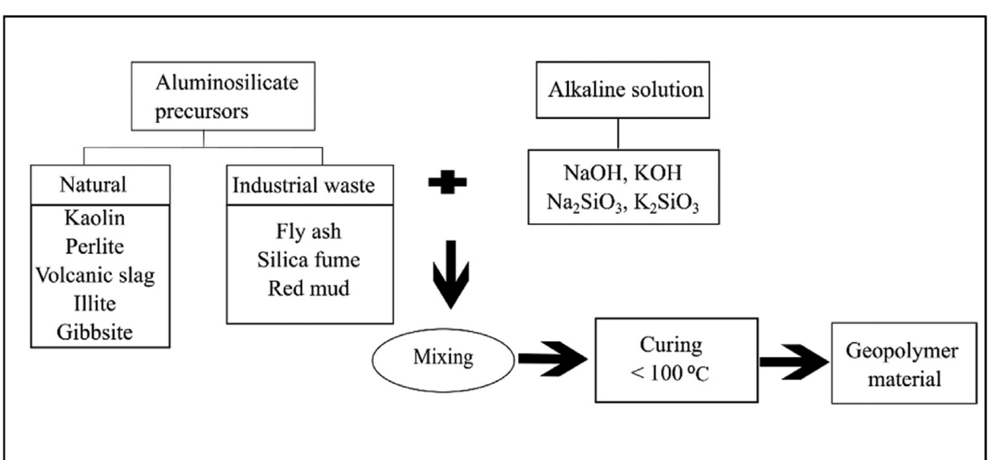

Fig. 7 – Steps of alkaline activation process [122].

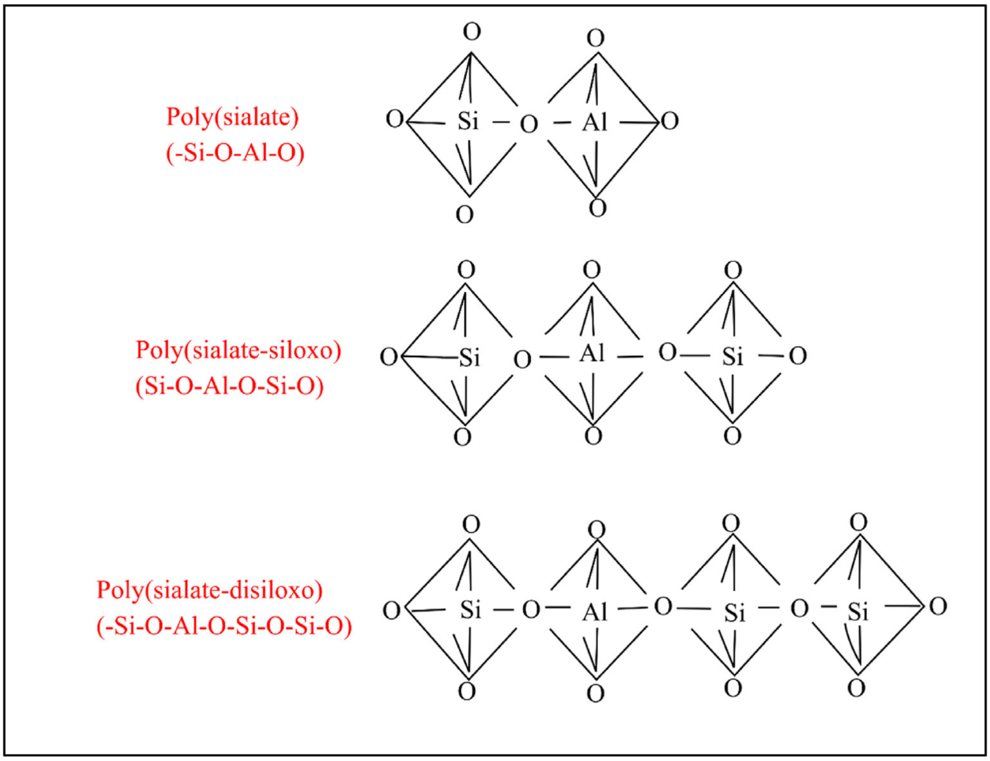

Fig. 8 – Types of geopolymer based in Si/Al ratio [123].

Dolomite $CaMg(CO_3)_2$ is a naturally occurring mineral rock made up of layers of calcium carbonate ($CaCO_3$) and magnesium ($MgCO_3$) carbonates [135–137]. Dolomite is a valuable mineral with good properties due to the presence of $CaCO_3$ and $MgCO_3$ plates in the crystal structure [138]. The concentration of CaO is highest in dolomite (33.4%), followed by MgO (17.1%), while SiO_2 and Al_2O_3 are slightly lower at about 2.5% and 0.7%, respectively [139,140]. Dolomite has excellent adsorption capacity than other mineral rocks such as sandstone [138,141]. Sorption of heavy metals on dolomite are controlled by kinetic reactions by the dissolution of dolomite. The dissolution of dolomite increases the pH of wastewater, which will be more effective for adsorption through the formation of bicarbonate ions [138,141]. Furthermore, dolomite has been discovered as a low-cost adsorbent for heavy metal ions with unique properties such as high surface area, cation exchangeability, and chemical alteration that can improve some of the natural material's undesirable characteristics. However, dolomite is rarely utilized in geopolymers because of its lower Si and Al content [142]. This is because Si and Al are the major constituents in the raw materials that will be used to develop geopolymers.

Besides, FA is a solid residue made up of small particles that are ejected from the boiler. According to the American Society for Testing and Materials (ASTM C618) [143] and the European Standard (EN 197-1 [144], FA can be classified as Class C or Class F based on the calcium oxide level. FA is primarily composed of high amount of 52.8% of SiO_2, 23.5% of Al_2O_3, 7.2% of iron oxide (Fe_2O_3) and 2.4% of CaO and has a high pozzolanic activity [117,118,145,146]. Besides pozzolanic properties, Class-C FA possesses some self-cementing qualities due to presence of its CaO concentration [75,92]. The presence of various metal oxide phases plays a significant function in this system since it leads to the increase in specific surface area [75]. As by product of coal combustion, FA are fine and glassy particles that can be collected in a variety of industrial processes. FA is dust that is expelled from the flue and gathered by the dust collector when raw coal is burned at extreme temperatures [147,148]. When coal is used as a fuel in the majority of industries, more FA is produced, causing numerous problems such as increasing land occupation while degrading the ecosystem and ecology [147–149]. FA as a filler increases the compressive strength, surface area, and catalytic sites of geopolymers [75,92]. Furthermore, the toxic metal ions are removed in large quantities from water through ion exchange and precipitation by metal complexation mechanisms due to the presence of oxygen atoms in the geopolymer matrix.

The main chemical compositions of slag are 55.1% of CaO, 22.8% of SiO_2, 10.6% of Al_2O_3 and 4.1% of MgO, making it an ideal raw material for geopolymer fabrication [150]. Slag can be divided into three types depending on the formation process, which are blast furnace slag (BFS), basic oxygen furnace slag (BOFS) and electric arc furnace slag (EAFS) [75]. BFS is the byproduct from Fe production. It is typically available in granulated, foamed, and pelletized forms depending on the cooling process. Ground granulated blast slag (GGBS) is initially in amorphous state when molten slag quickly solidifies during manufacturing process of pig Fe [148,151]. This substance is produced at temperatures of about 1500 °C and is fed with a carefully monitored blend of Fe ore, coke, and limestone [152]. When Fe ore is converted to Fe, the remaining elements form a slag that floats on top. This slag is tapped off as a molten liquid and rapidly cooled in vast quantities of water. Amorphous surfaces are commonly found on unstable face and the bonding has short range order and is unevenly formed, with each of the atomic species' positions is not randomly distributed in 3D orientation. Therefore, GGBS is highly reactive in the alkaline activation process [148,151]. GGBS is a good candidate for geopolymer production as it is made up of microscopic particles with high specific surface area. In addition, GGBS exhibits both cementitious (latent hydraulic activity) and pozzolanic (ability to react with $Ca(OH)_2$) properties [75,135].

In addition, sludge is a complicated substance that includes pathogens, organic contaminants, heavy metals, organic materials, and inorganic minerals [153]. Sludge also contains high concentrations of inorganic salts including inorganic ions (CO_3^{2-}, PO_4^{3-}, SO_4^{2-} and NO_3^-) and other elements such as (Si, Al, K, Na, Ca and Mg) [27,28]. In addition, sludge contains minor toxic heavy metal such as Zn, Pb, Ni, Cd and etc [154]. The chemical composition of sludge depends on the industrial process. This is because, the geothermal sludge contains 75.9% of SiO_2, 2.6 $Al_2O_3$and 0.4% of Fe_2O_3 [155], while tannery sludge is composed of 28.70% of Fe_2O_3, 4.5% of SiO_2 and 3.72% of Al_2O_3 [156]. In addition, sewage sludge has the main compositions of SiO_2 (52.8%), Al_2O_3 (18.5%) and Fe_2O_3 (11.2%) [157]. SiO_2, Fe_2O_3, and Al_2O_3 are the main inorganic components of sludge, which gives it the potential to be exploited as a renewable energy source [153]. Major limitations of sludge utilization are related to the potential of secondary pollution from heavy metals and also the high level of moisture [153]. But Li et al. [158] demonstrated that, although sludge materials are rich in heavy metals it is still considered as non-hazardous material. This is due to low leachability, mobility and accessibility of heavy metals from sludge before adsorption process. However, after adsorption process the leachability of heavy metal from sludge increased and thus it is considered hazardous material [29]. While, utilization of sludge based geopolymer in the adsorption might reduce the leaching of heavy metal from sludge. This is because, toxic elements from sludge can chemically bonding into amorphous 3D network of geopolymeric matrix [159].

Table 5 – Advantages and disadvantages of raw material for geopolymer synthesis.

Raw materials	Advantages	Disadvantages
Kaolin [123,167,168]	• Stable structure • High crystallinity • Lightweight • Strong and low cracking geopolymer	• Less reactivity • Low stability • Low porosity
Metakaolin [24,75,84,134,151,168,169]	• Effective encapsulation of hazardous materials • Mesoporous • High purity • High surface area • Different structural selectivity • Optimum sorption capacity • Best binding affinity • Multiple types of binding sites • Reduction of efflorescence	• Level of impurities • Inhibits particle mobility during mixing • Reaction system less workable • Weak rheological properties • High water demand • Quick hydration reaction
Dolomite [141,170,171]	• Excellent sorption capacity • Abundant • Flexible operation • Increase pH by dissolution of dolomite • Increased by bicarbonate ions • Cation exchangeability	• Non-porous material
Fly ash [92,95,172]	• Fine powders • Increase specific surface area • Good composite for geopolymer • More catalytic sites • O2-anionic endpoints with a high density	• More FA causing many problems • Less reactive • Rapid hardening and solidification
Granulated blast furnace slag [75,95]	• Highly reactive • Stability • High degree of pulverization • Hydrophilicity • Regeneration ability • Rapid geopolymerization • More heavy metal binding sites	• Very high processing temperature
Sludge [27,160,173]	• Closely resembles natural aluminosilicates • High concentration of inorganic salts • Contains non-toxic elements • Cation exchangeability • Reactive • Pozzolanic properties	• Contains toxic elements • Non-calcined sludge has undesirable properties

Based on leaching data, Guo et al. [159] found out that the heavy metal effectively immobilized in the geopolymer. Heavy metal leaching can be prevented by the formation of precipitates caused by anion interaction with heavy metals. Water treatment sludge (WTS), is a heterogeneous solid waste, which is high in Si and Al and closely resembles natural aluminosilicates. It can be turned into paste, mortar, and concrete [160–162]. WTS is referred to as inorganic sludge which is generated during purification of water. Formation of residue in the water treatment process by the addition of chemical reagents in the removal of fine particles and organic substances dissolution is called WTS. While, sewage sludge (SS) is a by-product of municipal wastewater after it undergoes biological treatment [163,164]. The chemical composition of sewage sludge ash is comparable to that of pulverized FA, with a high concentration of inorganic oxides such as SiO_2, Al_2O_3, and CaO which sometimes undergoes calcination process [161,165,166]. Calcination makes the sludge reactive, remove impurities and enhances pozzolanic properties, which improves the end product of geopolymer [160,164]. Additionally, it burns the organic material in the sludge, reducing the chance of internal geopolymer corrosion. Besides, the availability of Al during geopolymerization is enhance by calcination, which also accelerates the hardening of the geopolymer specimens. Meanwhile, others do not calcine the sludge to save energy or for the sake of convenience. The advantages and disadvantages of the each of the raw materials are tabulated in Table 5.

Table 6 presents the summary on raw materials used for geopolymer synthesis. Previous research by Cheng et al. [128] examined the adsorption ability of four different types of heavy metal ions (Cr^{3+}, Pb^{2+}, Cd^{2+} and Cu^{2+}) by MK based geopolymer. Selectivity of heavy metal ions for adsorption depending on the size of the hydrated ions, the free energy of hydration, and the activity of metal ions [89,111,174]. The affinity and force of attraction between hydrated cation and adsorbent influenced by the size of the hydrated cation and the affinity increases with decreasing hydrated radius. When the free energy of hydration in metals is increased, the number of heavy metal ions entering the adsorbent structure is decreased. In the case of Cr^{3+}, the number of hydrated ions, the free energy of hydration, and the activity were greater than those of other metals. Despite the fact that Cr^{3+} should have a better adsorption, a longer soaking time of geopolymer releases more alkali, raising the pH of the solution. As a result, the geopolymer's capacity to remove Cr^{3+} was reduced as a result of alterations in the ionic species. Thus, the adsorption of Pb^{2+} is optimal compared to other metal ions. Besides, the leaching ability of Cr^{3+} was highest due to unbalance net charge. Whereas Pb^{2+} has low possibility of leaching as it entrapped into locked into pores. Nevertheless, it will be

Table 6 – Raw Materials for geopolymer synthesis.

Author	Materials	Targeted metal ions	Qmax(mg/g)	Findings
Cheng et al. [128]	• MK	• Pb^{2+} • Cu^{2+} • Cr^{3+} • Cd^{2+}	100	• Optimum adsorption of Pb^{2+} occurred in MK based geopolymer • Pb^{2+} activity is increased by increasing its mobility in aqueous solution
Panda et al. [55]	• Pyrophyllite mine	• Co^{2+} • Cd^{2+} • Ni^{2+} • Pb^{2+}	0.114–17.54	• Geopolymer pyrophyllite becomes an effective adsorbent for metal ions than raw pyrophyllite • The adsorption process is endothermic, it becomes more favourable as the system temperature rises
Andrejkovičová et al. [133]	• MK • Zeolite	• Pb^{2+} • Cd^{2+} • Zn^{2+} • Cu^{2+} • Cr^{3+}	7.76–261.22	• 50:50 ratio of MK and zeolite was the optimum ratio for producing high strength geopolymer products • Pb^{2+} was adsorbed in very high amounts by all geopolymers
Hu et al. [76]	• MK • RET • SF	• Pb^{2+} • Ba^{2+}	1.1–1.4 (mg/L)	• 20% addition of RET improved the structural strength of the developed geopolymer matrix • RET based geopolymer was capable of effectively immobilizing heavy metal cations
He et al. [22]	• FA	• Pb^{2+}	166.40–253.80	• FA geopolymer was successfully transformed into various zeolites through hydrothermal conversion • Adsorption capacity of philipsite was higher than the other zeolites.
Wang et al. [175]	• RD • Coal gangue	• Pb^{2+} • Cu^{2+}	90–137.7	• The geopolymerization process with incorporation of RD, increased the specific surface area and influenced the adsorption performance • The geopolymers demonstrated superior leaching resistance and high heavy metal solidification capacity compared to others

better if this study could provide the analysis of zeta potential (ZP) at which it provides important information on the electrostatic interaction between adsorbent and adsorbate.

On the other hand, Panda et al. [55] focused on the preparation of pyrophyllite mine waste based geopolymer and explored its effectiveness in the application of heavy metal adsorption such as Co^{2+}, Cd^{2+}, Ni^{2+} and Pb^{2+}. After geopolymerization process, swelling was formed in the synthesized geopolymer with varied shape and size. In the topmost layers, these swellings caused exfoliation that looked like flakes or scales. These swellings may have grown to their maximum size then collapsed, leaving voids or holes as revealed in Fig. 9. The porosity of the material is increased by these voids and enhanced the adsorption capacity of geopolymer. In comparison to pyrophyllite, the geopolymeric pyrophyllite has much higher adsorption capabilities for all of the metal ions under study, showing that it is a more effective adsorbent. In pyrophyllite based geopolymer, the removal efficiency of Cd^{2+} was highest among other metal ions whereas the removal efficiency of Pb^{2+} was higher in pyrophyllite sample. This difference contributed to variations in the surface characteristics during geopolymerization. Nevertheless, a study on the regeneration ability of pyrophyllite based geopolymer was not identified although it is an important element in evaluating the performance of the adsorbent.

A research conducted by Andrejkovičová et al. [133] explored the effect of natural zeolite addition as a filler in MK based geopolymer. The geopolymer samples were prepared by replacing MK with zeolite at different percentages of 0, 25, 50 and 75%. 100% of MK geopolymer contained pores with large diameter and thus it reaches highest value of water absorption and surface area. Incorporation of zeolite into as a filler in MK based geopolymer cause a decline in the water absorption and surface area. In accordance with that, highest adsorption capacity of Cu^{2+} and Cr^{3+} was attained at 100% MK geopolymer while at 75% MK geopolymer the adsorption capacity of Pb^{2+}, Cd^{2+} and Zn^{2+} was maximum. The adsorption has been greatly enhanced when the amount of MK in the structure increases due to a clearly higher degree of geopolymerization. MK based geopolymer has higher rate of adsorption and thus the adsorption process did not require a longer period of time. In addition, greater surface area of MK increase surface area and results in more available sites for heavy metal adsorption. However, in this study the raw materials used in this study were not subjected to FTIR analysis in order to determine the chemical functional groups which have a main role in the adsorption of heavy metals through chemisorption.

In year 2020, Hu et al. [76] prepared rare earth tailing (RET) based geopolymer for immobilization of heavy metals ions such as Pb^{2+} and Barium (Ba^{2+}). At the beginning of the geopolymerization process, certain amount of NaOH was added in deionized water, followed by addition of SF to the solution and stirred for 3 min at 600 r/min to fully dissolve. Thereafter, MK with 20% of RET was mixed with the prepared alkaline activator and the obtained geopolymer paste was cured at 60 °C for 8 h. To determine the immobilization performance of heavy metal ions, lead nitrate $Pb(NO_3)_2$ and barium nitrate $Ba(NO_3)_2$ were mixed with RET based geopolymer. During the geopolymerization process, additional Pb^{2+} and Ba^{2+} chemically with the reactive components and this can be confirmed by observing the X-ray diffraction (XRD) peaks corresponding to PbO and $BaSiO_3$. Besides, introduction of heavy metal cations caused a change in the extranuclear electron distribution of Si/Al and an increase in non-bridged oxygen. As a result, Na^+ was partially replaced by Pb^{2+} and Ba^{2+} and then immobilized in the framework of [T-O-Na^+-O-T] where T: Si or Al as shown in Eqs. (1–4). In addition, the concentration of leachate increased slightly with the increasing amount of Pb^{2+} and Ba^{2+} at the range 0.2–1.0 wt.%. However, the influence of other important variables such as time, temperature and pH on the leaching ability of Pb^{2+} and Ba^{2+} from RET based geopolymer were not discussed in this work.

$$SiO_2.Al_2O_3 + 3OH^- + 3H_2O \rightarrow 2[Al(OH)_4]^- + [SiO_2(OH)_2]^{2-} \quad (1b)$$

$$Y^{2+} + 2OH^- \rightarrow Y(OH)_2 \quad Y : Pb^{2+} \text{ or } Ba^{2+} \quad (2)$$

$$[Al(OH)_4]^- + [SiO_2(OH)_2]^{2-} + Pb(OH)_2 \rightarrow -[Al-O-Pb-O-Si]_n- \quad (3)$$

$$[Al(OH)_4]^- + [SiO_2(OH)_2]^{2-} + Ba(OH)_2 \rightarrow -[Al-O-Ba-O-Si]_n- \quad (4)$$

Moreover, He et al. [22] derived various zeolites from circulating fluidized bed FA based geopolymer via hydrothermal conversion to adsorb Pb^{2+} from wastewater. First of all, Na-geopolymer based on FA with 1:1 (Si/Al) molar ratio was produced. Then, 10 g of granular Na-geopolymer sample was put in a beaker which is filled with 100 mL of 1 M aqueous

Fig. 9 – Formation of swelling in pyrophyllite based geopolymer [55].

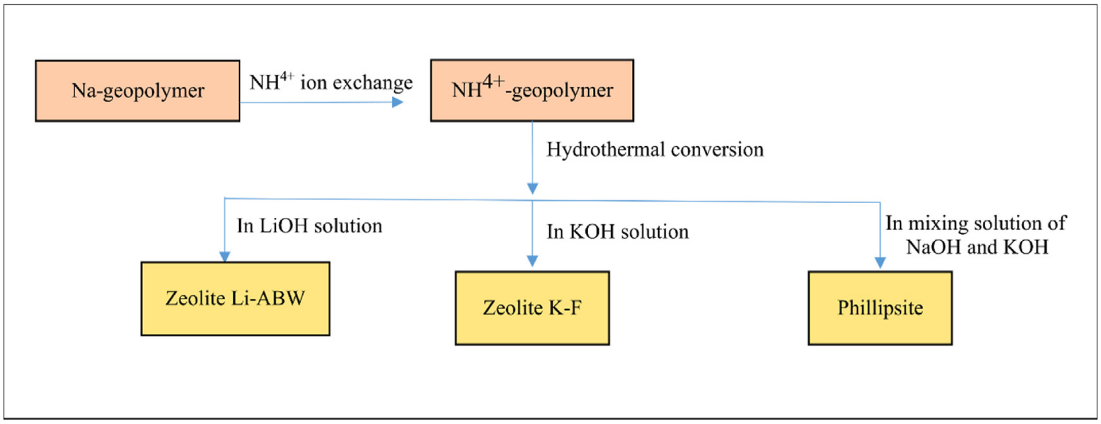

Fig. 10 – Topological structures of synthesized zeolites [22].

ammonium nitrate (NH_4NO_3) solution and stirred for 2 h at 70 °C in order to remove Na^+ from geopolymer by ammonium (NH_4^+) ion exchange reaction. After that, the NH_4^+ geopolymer was converted into various zeolites such as LiOH based zeolite (Li-ABW), KOH based zeolite (K–F) and NaOH and KOH based zeolite (Phillipsite) by hydrothermal conversion as illustrated in Fig. 10. FA geopolymer was successfully converted into three types of zeolites according to the synthesizing condition. Based on the XRD pattern obtained, Pb^{2+} adsorption does not change the zeolite structure of Li-ABW. While, appearance of new peaks related to $PbSiO_3$ in phillipsite and Pb_5Si8O_{21} in K–F after adsorption indicating participation of surface chemical reaction during adsorption process. Nevertheless, it would be helpful for future researchers if the adsorption experiment of Pb^{2+} by geopolymer is conducted in order to compare the adsorption capacities of Pb^{2+} by geopolymer and zeolites produced.

In addition, Wang et al. [175] found out the relation between geopolymer gel and its heavy metal adsorption performance by utilizing industrial wastes such as coal gangue (CG) and RD in the synthesis of geopolymer. Participation of sodium silicate (Na_2SiO_3) and sodium aluminate ($NaAlO_2$) activators in the synthesis of CGRD based geopolymer increased the geopolymerisation process, formation of gel amount and thereby increased the adsorption capacities of metal ions. More compact gel structure was formed with the contribution of $NaAlO_2$ (NaAl-CGRD) whereas ordered gel structure with formation of porous and increased specific area was obtained with involvement of Na_2SiO_3 (NaSi-CGRD) as presented in Fig. 11. Moreover, batch adsorption experiment for removing heavy metal ions was performed at various experimental variables including initial metal ion concentration, pH, and contact time at constant temperature. Nonetheless, this work neglected the information on the constant temperature used at 30 °C for the adsorption test.

Different raw materials produce distinct reaction products, chemical linkages, and microstructural development depending on the reactive phase present [176]. Apart from choosing suitable raw materials, deciding the optimum parameters for the geopolymer synthesis is also vital in order to ensure that the synthesized material meets the needs of application. This is because, synthesis parameters do not only influence the framework, structure and properties of the formed geopolymer but also directly influence the performance of the heavy metal adsorption [118,177,178].

4.3. *Synthesis parameter of geopolymer*

Molar concentration of alkaline activator, alkaline activator ratio, solid to liquid ratio (S/L) and curing temperature are the most important parameters in the alkaline activation process. Molar concentration of alkaline activator plays an important role in the complete dissolution of aluminosilicate precursors [177,178]. S/L ratio controls the homogeneous mixture as it

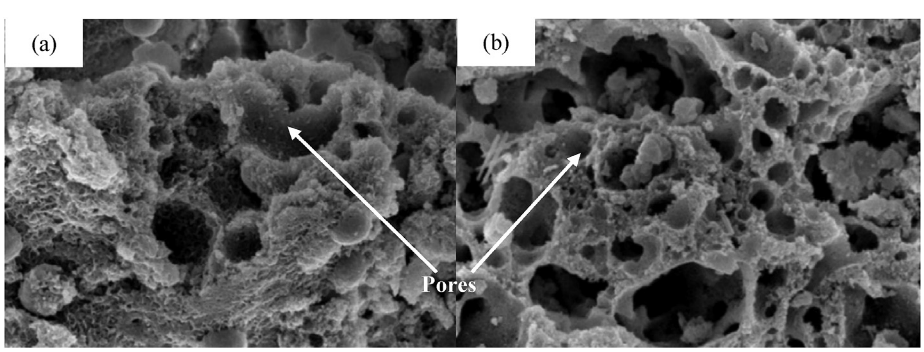

Fig. 11 – Morphology of (a) NaAl-CGRD (b) NaSi-CGRD based geopolymer [175].

directly influences the workability and hardened strength of geopolymer. Whereas alkaline activator ratio determines the rheology, pore-forming process as well as degree and speed of geopolymerization [134,179]. Moreover, curing temperature will aid in the dissolution of Si and Al in the precursor, promote polycondensation and strengthen the geopolymer paste formed [176,180]. Thus, these parameters are need to be preciously controlled to obtain synthesized geopolymer with desired properties.

4.3.1. *Molar concentration of alkaline activator*

The type and concentration of alkali solution influence the dissolution of aluminosilicate material. In the production of geopolymer, alkali hydroxide plays two important roles [55,177]. Firstly, it activates the precursor by releasing reactive species for geopolymerization. Second, the alkali metal acts as a structure-forming element and balances the negative charge of Al^{3+} in IV-fold coordination. 1/2 mol M_2O (Na/K) is required for 1 mol IV-fold coordinated Al^{3+} in order to achieve neutrality [181]. As a result, the M_2O content has a significant impact on the rate and extent of the polymerisation reaction as well as the final product stabilisation. The dissolving of aluminosilicate sources necessitates the use of alkali hydroxide. This is because the presence of OH^- ion catalyzes the activation of the precursor by dissolving the reactive ions, and the alkaline metal thereby forming part of the polymeric structure [59,182,183]. The leaching of Si^{4+} and Al^{3+} ions are significantly greater in NaOH solution compared to potassium hydroxide (KOH) solution and the amount of leaching depends on the concentration of NaOH and the reactivity of aluminosilicate material [176,178]. Thus, the molarity of sodium hydroxide is crucial during the planning of a soluble activator. Increasing the molarity of NaOH increases the amount of NaOH, which affecting the Na_2SiO_3/NaOH ratio. Increasing NaOH content resulting a drop in Na_2SiO_3 content [184]. At high NaOH concentration, increase in the Na_2O content promote the dissolution of silica and alumina from the raw material [80]. As a result, more dissolved ions from silicon and alumina are used in the synthesis of geopolymer, resulting in a denser 3D and stronger geopolymer. However, excessive concentration of NaOH will cause early precipitation of silicate products due to excessive OH^- and reduces the dissolution of aluminosilicate material due to the increase in Si coagulation. This is because, Si^{4+} ions will leach out faster than Al^{3+} ions resulting in the formation of more tetrahedral oligomeric SiO_4 than AlO_4 [55,185]. Besides, high NaOH concentration will also increase the boiling point of the NaOH solution, hindering the evaporation of water in the mixed slurry and thus affecting monomer polycondensation [179,186]. In addition, the thickening of the solution caused by a greater NaOH concentration resulted in lesser moving ions from the solid raw material, preventing additional ion leaching [134,176].

4.3.2. *Alkaline activator ratio*

During the synthesis of geopolymer, alkaline activator is another crucial element. By the addition of alkaline activator to aluminosilicate materials, $[SiO_4]^{2-}$ and $[AlO_4]^{2-}$ tetrahedrons can staggered and overlapped to produce geopolymer with 3D network structure through the process of "solution-monomer-reconstruction-polycondensation". The combination of NaOH and Na_2SiO_3 is preferred for alkaline activation, as using only NaOH as an activating solution has some disadvantages such as it is corrosive in nature and releases a lot of heat during dissolution of aluminosilicate materials [177,187]. Whereas employing the Na_2SiO_3 simply as an activating solution does not yield the dissolved species required to construct the alumino-silicate framework as it lacks enough OH^- ions [182,183]. NaOH and Na_2SiO_3 are the most commonly used alkaline activator compared to KOH and potassium silicate (K_2SiO_3) as NaOH has better leaching ability and greater charge density compared to KOH which are related to the smaller size of Na^+ and thus it can move freely through the gel [188–190]. This permits Na^+ to better stabilize the silicate monomers and dimers in the solution, enhancing the dissolution rate of source material. The alkaline activator ratio is referred to the ratio of Na_2SiO_3 to NaOH (SS/SH) [123,191]. The high SS/SH ratio can improve polymerization and result in a more compact silicon-rich gel phase due to the presence of more Si ions in the solution. As the relative SiO_2 content rises, the pH value falls, and the viscosity rises [134,192]. Low pH value limits the reaction with silicate compounds and slow hydration rate will result in low strength. However, at lower alkali activator ratio, the Na_2O content and pH increase and the viscosity of geopolymer paste decreases. The high concentration of Na_2O improved the dissolution of Si-Al raw materials. Alkaline environment produces more products and increases the hydration rate and strength [134,192]. Formation of crystals occurs in the environment with low levels of alkalinity, but they cannot form in environments with excessive levels of alkalinity. Thus, the appropriate ratio of alkaline activator is required for effective geopolymerization and uniform gel formation.

4.3.3. *S/L ratio*

The S/L ratio is equivalent to the aluminosilicate precursor-to-activator solution ratio. The dissolution process of aluminosilicate source and also the subsequent reaction will be influenced by the properties of the solid aluminosilicate. However, the dissolution of the solid raw material, determination of structural break and recombination and also the polycondensation process will be influenced by the alkaline activator [134]. In addition, S/L ratio determines the modulus ratio of Al_2O_3/Na_2O at which Al_2O_3 comes from the aluminosilicate source while Na_2O comes from the alkaline activator solution. At low S/L ratio, the dissolution of aluminosilicate materials is accelerated by the presence of excess Na_2O in alkaline solution [181,193]. However, excess alkaline activator delays the reaction of geopolymerization and required longer coagulation time. This can be further explained by the less contact between alkaline activator and reacting materials. There is more fluid medium than solid content in the mix, and the contact between the activating solution and the reacting materials was far and limited [123,194]. Thus, the dissolution of aluminosilicate materials is believed to slow as the alkaline attack start from outer surface of material. In addition, the extra Na^+ ions in the goepolymer mix with increasing liquid ratio will disrupt the equilibrium charge of polymer framework, weaken the structure formed and degrade the strength of the geopolymer [123,176]. On the other hand, increasing S/L ratio increases the modulus ratio of Al_2O_3/Na_2O. At higher S/L ratio increased solid precursors do not dissolve properly due to the lack of alkaline solution in the matrix resulting in the inefficient hydrolysis reactions and gel formation [176]. Besides, the ratio of SiO_2/Al_2O_3, which is coming from aluminosilicate solid precursors is directly proportional to the setting time of geopolymer [66]. The larger the ratio of SiO_2/Al_2O_3, the prolonged the setting time. Silicate species is required for the quick exchange and oligomerization reaction between the aluminate and silicate species from the kaolin. But, increasing S/L will increase the Si content in the system as it causes oligomer size to rise, which impacts the kinetics of SiO_4 unit exchange across species during geopolymerization [181,195,196].

4.3.4. *Curing temperature*

Curing process for geopolymers involves two steps, which are dissolution of precursors and condensation period [134,180]. Four steps of the condensation phase are speciation equilibrium, gelation, rearrangement, and polymerization. Thus, the temperature and time are critical factors in curing because it is responsible for facilitating hydrolysis, condensation process, and strengthening the geopolymer paste [180,197]. Different curing procedures have a significant impact on the long-range order of tetrahedrons during the geopolymer polycondensation reaction, as well as the pore structure [91]. The polycondensation process is aided by a higher curing temperature, which allows for more efficient alkaline attack on the precursor, increasing the amount of reactive product produced and the compactness of the geopolymer [134,198]. High curing temperature increase the mobility of Na^+ and OH^- ions and leads to the development of extremely dense sodium aluminosilicate crystal which is responsible for higher strength [199]. Besides, the polymerization reaction is more powerful at higher curing temperature, transforming 2D polymer chains into 3D polymer chains with a stronger bond. In addition, the degree of reaction becomes stronger at the high curing temperature and increases the total pore volume and surface area. However, a constant increase in curing temperature might affect the geopolymerization process by quick loss of water and formation of microcracks [134,199]. In addition, a greater temperature could facilitate flash setting, which would stop additional ion leaching and reduce the Si/Al ratio of cured geopolymer. For sample cured at a higher temperature, a longer curing duration is not a desirable condition [199]. This is because, geopolymerization is an exothermic reaction and the discharge of Na^+ and OH^- ions from the alkaline activator and the development of the bond with the Si and Al ions mostly depends on the curing temperature. But curing at high temperature for longer period will destroy the granular structure of geopolymer gel due to thermolysis of -Si-O-Al-O bond and also leading to dehydration and excessive shrinkage [134,199]. Longer curing period is only desirable for the sample cured at lower temperature. Thus, adequate curing is required to accelerate and complete dissolution and condensation of Si and Al species.

Table 7 – Synthesis parameter of geopolymer adsorbent.

Authors	Material	Parameters	Targeted metal ions	Qmax(mg/g)	Findings
Kara et al. [200]	MK	• 80 °C for 2 days	• Mn^{2+} • Co^{2+}	69.23–72.34	• Mn^{2+} ions have greater adsorption than Co2+ ions due to more negative ZP • Mn^{2+} and Co^{2+} adsorption by MK based geopolymer was caused by more than one mechanism
Darmayanti et al. [118]	FA	• 7 M KOH • 7 M NaOH • 3.5 M Na2SiO3 • 85 °C for 1 day	• Cu^{2+}	7–40	• The maximum adsorption capacity of NaSi-GP was *greater* than KSi-GP, Na-GP and K-GP due to more organized structure • Due to faster hydrolysis and condensation reaction than K^+, Na^+ forms more ordered structure
Ghani et al. [201]	Clay	• 6 M KOH • 80 °C for 1 day	• Ni2+ • Co^{2+}	500–520	• Both heavy metal ions have an inhibitory impact on each other in a competitive adsorption study • The adsorption process remained physisorption, based on the low Ea value calculated
Lan et al. [202]	Coal FA MK	• 80 °C for 16 days	• Pb^{2+} • Cd^{2+}	78.2–164.1	• In *high* alkaline environments, the conversion of geopolymers to zeolites is accelerated • 0.8-FAMKG has higher adsorption –desorption isotherms, specific area and pore volume than 1.2-FAMKG
Wei et al. [203]	MK	• 11 M *NaOH* • (65–105 °C) • (5 min-72 h)	• Pb^{2+}	308.30–529.67	• NaA structure had maximum adsorption capacity which was faster than SOD and SOD + NaA • Adsorption process of Pb^{2+} by NaA and NaA + *SOD* occurs in 3 stages while by SOD, only 2 stages involved

Table 7 presents the summary of synthesis parameters for geopolymer synthesis. In 2018, Kara et al. [200] studied the optimum conditions for Mn^{2+} and Co^{2+} adsorption by MK based geopolymer for the first time in both batch and continuous system. For the batch system, parameters such as initial pH, temperature, adsorbent dosage and initial metal ion concentration was evaluated. While, adsorbent amount, flow rate and reuse potential were tested in continuous system. The synthesized geopolymer adsorbent produced rather high adsorption yields in both batch and continuous processes. In addition, synthesized geopolymer adsorbent does not require solution pH modification during adsorption process. Besides, a short period of time is required to attain the adsorption equilibrium, and temperatures above 30 °C have no impact on the adsorption yield. On the other hand, in a continuous system, the geopolymer also provided excellent metal ion removal at high flow rates. However, Kara et al. [200] study failed to reveal some important parameters used in the geopolymerization process such as molarity of NaOH concentration, S/L ratio, and SS/SH ratio, which directly influence the structure and framework of the geopolymer. In addition, the adsorption mechanisms involved in the adsorption process of Mn^{2+} and Co^{2+} by MK based geopolymer were electrostatic interaction, ion complexation between heavy metal ions and functional group of geopolymer adsorbent and ion exchange mechanism between heavy metal ions and alkali metal.

Moreover, Darmayanti et al. [118] explored the impact of alkali activation on structural changes of FA based geopolymer and its impact on adsorption capacity of Cu^{2+}. Alkali activation of FA using NaOH + Na_2SiO_3 (NaSi-GP) obtained larger specific area than KOH + Na_2SiO_3 (KSi-GP), KOH (K-GP) and NaOH (Na-GP). Thus, NaSi-GP obtained the greatest adsorption ability of Cu^{2+} due to the structural modification during geopolymerization. Structural change can be more precisely directed by Na^+ than by K^+. Introduction of Na^+ speed up the hydrolysis and condensation reaction more quickly than K^+ and results in more ordered structure in NaSi-GP. On the other hand, the higher ionic radius of K^+ create a steric obstacle during the structural modification. In addition, based on the scanning electron microscope (SEM) analysis, FA is made up of spherical particles with large particle size. It is also mentioned that the morphology of FA undergoes structural modification upon alkaline activation by NaOH and KOH. The surface of the primary particles made of FA is covered by worm-like nanoparticles from the additional silicate in NaSi-GP and KSi-GP. The formation of worm-like particles was caused by alkali treatment of amorphous silica. However, the images provided by SEM analysis did not match with the labelling of the figure. Thus, it would have been more comparable and understandable if the pictures were standardized based on the types of alkaline activation.

In another study, Ghani et al. [201] developed low-Fe lateritic clay based geopolymer to adsorb $Ni2^+$ and Co^{2+} from aqueous solutions. Based on the SEM, the adsorption of metal ions was confirmed by the covering of surface pores and cavities, as well as changes in the surface morphologies of the geopolymer based adsorbent upon adsorption as expressed in Fig. 12. Moreover, the peak position, intensity, and shape of all characteristic peaks in FTIR before adsorption were changed significantly after adsorption due to accumulation of heavy metal ions on the adsorbent's surface. However, the XRD patterns of the adsorbent after adsorption were not revealed to support that there is no formation of new crystal structures through chemical reactions.

In contrast, Lan et al. [157] used FA and MK as aluminosilicate material in the preparation of geopolymer for the adsorption of heavy metal ions. At the beginning of the process, two molar ratios of (SiO_2/Na_2O) were used in the mixing process of alkaline activator which are SiO_2:Na_2O = 0.8 and SiO_2:Na_2O = 1.2. Then, the geopolymer paste was made by mixing 35% of FA and 65% of MK with prepared alkaline activator SiO_2:Na_2O = 0.8 (0.8-FAMKG) and SiO_2:Na_2O = 1.2 (1.2-FAMKG) respectively. The obtained geopolymer paste was then dried, crushed and sieved to obtain fine particles of geopolymer. Due to the presence of significant geopolymer gels in both 0.8-FAMKG and 1.2-FAMKG, some Pb^{2+} and Cd^{2+} could be permanently fixed in the tetrahedral structure. Nonetheless, it should be noted that, in this work it was not mentioned why the percentage of raw materials was set at 35% of FA and 65% of MK as the optimum parameter to conduct the experiment on the adsorption ability of heavy metal ions without any validation.

In the year 2022, Wei et al. [203] prepared three types of geopolymer zeolite microsphere (GZM) from MK by using

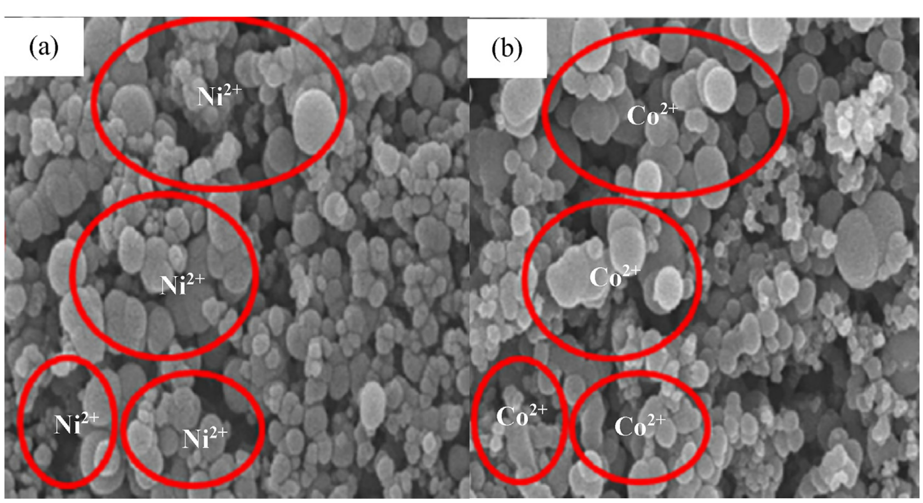

Fig. 12 – SEM image of adsorbent (a) Ni^{2+} and (b) Co^{2+} after adsorption [201].

suspension dispersion solidification and in-situ conversion method as illustrated in Fig. 13. The three types of GZM (Zeolite (NaA), Sodalite (SOD) and SOD + NaA) were obtained by altering the parameters such as sodium oxide to alumina oxide ratio (Na_2O/Al_2O_3), water to sodium oxide ratio (H_2O)/(Na_2O), curing temperature and curing period. The optimal Na_2O/Al_2O_3 to prepare GZM was 1.9. As n(Na_2O)/n(Al_2O_3) ratio was increased, the sphericity of the microsphere adsorbent steadily improved, and the average microsphere particle size significantly decreased with a more uniform particle size distribution due to accelerated dissolution of Si and Al through alkaline environment. When the H_2O/Na_2O ratio was 12 and the curing temperature was between 65 and 85 °C, the microsphere sphericity was better and particle size was smaller with a uniform distribution. On the other hand, different curing times had no impact on the sphericity of GZM, it had a considerable impact on the surface structure. However, only using NaOH as alkaline activator has some drawbacks such as being corrosive and releasing a lot of heat during the dissolution of aluminosilicate material.

Nevertheless, powdered geopolymer adsorbent cannot stand alone in remediation application as it has difficulty in recovery [204–206]. Thus, adsorbents require support materials such as porous ceramics or polymer foams to allow it to be used in industrial application. Porous geopolymer has become efficient adsorbent in wastewater remediation compared to other types of adsorbents such as conventional geopolymer and pervious geopolymer [122,128]. More binding sites are provided by the porous structure of geopolymer, which enhance the permeability, increase mass transfer, and lower the pressure drop [128,204].

5. Modification technique on geopolymer adsorbent

In general, geopolymer pores can be classified into four length scales which are Level I (Macro pores), Level II (Meso and Micropores), Level III (Nano pores) and Level IV (Molecular pores) [91,207] as illustrated in Fig. 14. Macro pores are known as bubble pores with typical size greater than 10 μm. The geopolymerization process, composition, and curing condition including high viscosity, high-speed mixing, insufficient debubbling, and forceful heating can all considerably increase the content of macroscale pores [91]. Mesopores and micropores are pores with a diameter of 100 nm to 10 μm that are made up of microcracks, hollow voids inside or around the unreacted particles. These pores are formed by the presence of unreacted particles in geopolymer binder, which is caused by the deficient alkali, insufficient curing time and chemical reactivity of raw materials [208,209]. Moreover, nano pores are in the range between 2 and 100 nm and present abundantly in geopolymers. The pores in low calcium content geopolymers are finer than high calcium content geopolymers. Geopolymers with high calcium concentration have a more complex pore structure and there is no distinctive pore size and the pore size distribution is wider [91,210]. However, molecular pores less than 2 nm are usually present in the aluminosilicate network, evident by the presence of small rings and cage structure. Molecular pores are influenced by the Si/Al ratio and structural disorder of the aluminosilicate network [91,211,212]. Therefore, the geopolymer synthesis in an aqueous medium enables custom-tailored porosity. Various techniques were employed to achieve desired porosity for various purposes [90,205,213]. Several methods for producing macroporous ceramics have been reported, including the use of a replica, sacrificial template and direct foaming method [122,205,213].

In addition, thermal and mechanical processes are physical modification methods, which improve the physical characteristics of adsorbent such as surface area, pore volume, density and solubility [214,215]. For instance, changes in physical properties include density, pore structure and microstructure occur in geopolymer based adsorbents with the formation of cracks upon heat treatment at elevated

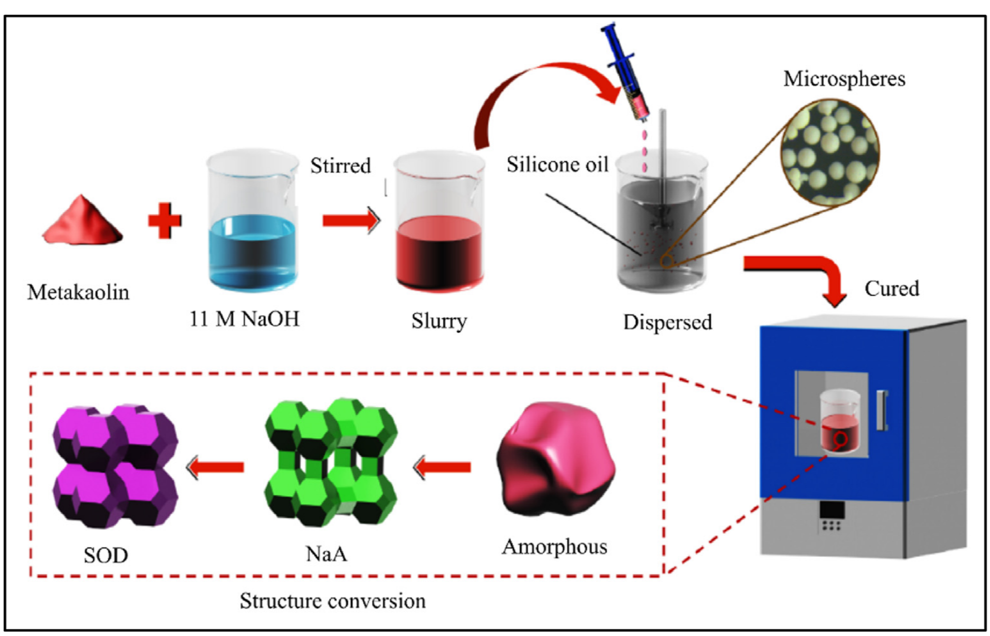

Fig. 13 – Production of GZM adsorbents [203].

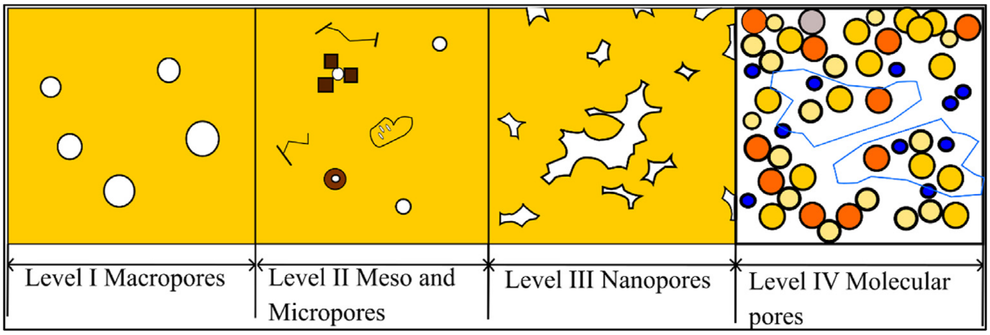

Fig. 14 – Types of geopolymer pores [91].

temperature [214,216]. There are three stages to the thermally induced pore structure change in geopolymer pastes as shown in Fig. 15: (i) At 100 °C, the percentage of mesopores of geopolymer decreased by further geopolymerization, which provides healing effect on pore the structure [216]. (ii) In contrast, when the geopolymer is subjected to a temperature in the range between 100 and 600 °C, severe cracks are exhibited in the matrix, which are strongly related to evaporation of free water and chemically bonded water and the decomposition of binder gel [216]. This further destruct the geopolymer matrix and increases the pore connectivity by enlarging the initial cracks which also results in the rise in the pore size. Pressure builds up causing the microcracks to expand and to crack much more [217,218]. Formation of microcracks will aid in the heavy metal adsorption by diffusing through the cracks or pores into the particles [167,219]. (iii) However, thermal treatment beyond 600 °C significantly reduced the presence of mesopores by refining the pore structure [216]. On the other hand, in terms of chemical transformation upon heat treatment, geopolymer is chemically stable from room temperature till 600 °C, while considerable changes in crystalline phases is observed after exposure to 800 °C with the formation of nepheline ((Na, K)$AlSiO_4$) as the result of sodium aluminosilicate hydrate (N-A-S-H) gel crystallization [220]. However, the main drawback of this approach in the modification of geopolymer adsorbent is the loss of thermally unstable functional groups at higher temperatures [123,221]. As a result, the production of chelates with metal species reduces, resulting in fewer metal ions adsorption.

Besides, high-energy ball milling is a mechanochemical method, which can be used for obtaining nanomaterials with enhanced material properties such as specific surface area, homogeneity, and dispersion [222–224]. Mechanochemical refers to the combination of basic solid-state approach and mechanical energy input, which includes applying pressure on surface-bound compounds to promote kinetic reactions between solids [225,226]. During collision, powder particles caught between the surfaces of colliding milling tools are subjected to rapid mechanical loading at relatively high strain rates resulting in local mechanical stresses that are unevenly distributed across the network of particle interactions as shown in Fig. 16 [226]. The granular bed undergoes rearrangement under the influence of mechanical forces, characterized by particle compression as the surfaces slide against each other and the onset of severe mechanical deformation [226]. Local deformations enable the activation of mechanochemical transformations, which then occur

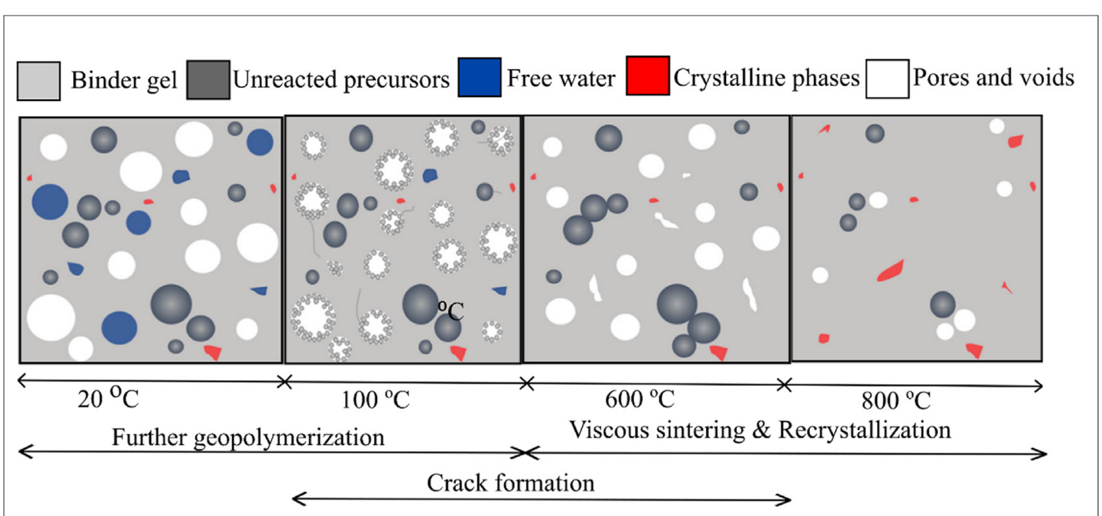

Fig. 15 – Thermal treatment on FA based geopolymer at [216].

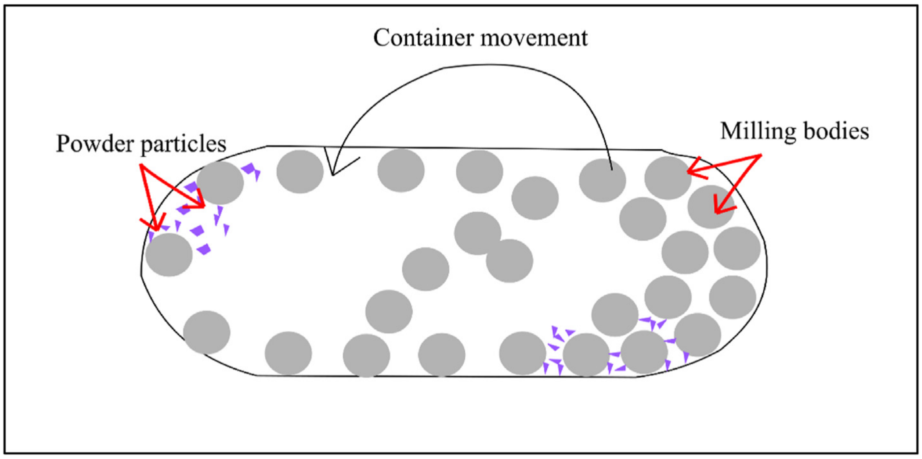

Fig. 16 – Milling mechanism in high energy ball milling.

at individual collisions under processing circumstances. The advantages of the ball-milling technology include convenience of use, low cost, and environmental friendliness, as it is able to enhance the properties of the material produced without the presence of chemical reagents [222,223,227]. High-energy milling does not only participate in improving surface structure of adsorbent, but also induces significant physicochemical changes in milled materials [228]. During this process, the induced high energy impact is able to break the chemical bonds, diminish crystallinity, enhance amorphization and also increase the density of surface functional groups in solid materials, which can potentially improve the adsorption performance of adsorbent [226,228]. Previous researchers reported that, ball-milled materials have been widely used in the

Table 8 – Preparation of porous geopolymer adsorbents.

Authors	Raw material	Source/Method	Pore size (nm)	Targeted metal ions	Qmax (mg/g)	Findings
Ge et al. [231]	• MK	• H_2O_2 foaming agent • K12	2–160	Cu^{2+}	52.63	• Typical structure of geopolymer did not change upon preparation of porous geopolymer sphere • Prepared porous geopolymeric sphere has relatively low adsorption ability compared to powder adsorbents
Duan et al. [90]	• FA • IOT	• H_2O_2 foaming agent	10–110	Cu^{2+}	113.41	• Formation of porous structure through transformation of FA and Fe ore tailing into an amorphous foaming geopolymer • Porous geopolymer increases available sites for Cu^{2+} binding and thereby increasing adsorption ability
Hu et al. [232]	• $CaCO_3$	• Ball milled	–	Cu^{2+}	99.76	• Cu^{2+} removal through chemical precipitation rather than physical adsorption • 10% of ball volume become optimum to clear the effluent discharge limit of Cu
Tan et al. [206]	• FA • Calcined clay	• H_2O_2 foaming agent	17.58–56.47	Ni^{2+}	19.94	• Adsorption performance towards Ni^{2+} increases with increasing pore size and network • An open network structure acts as a liquid penetration channel and lowers the penetration resistance
Pachana et al. [219]	• WTR	• Aluminium • Powder • Propylene glycol	–	Fe^{2+} Mn^{2+}	100%	• After 24 h of immersion, the Fe is completely removed using a geopolymer which calcined at 400 °C • Adsorption rate of Fe was higher than Mn

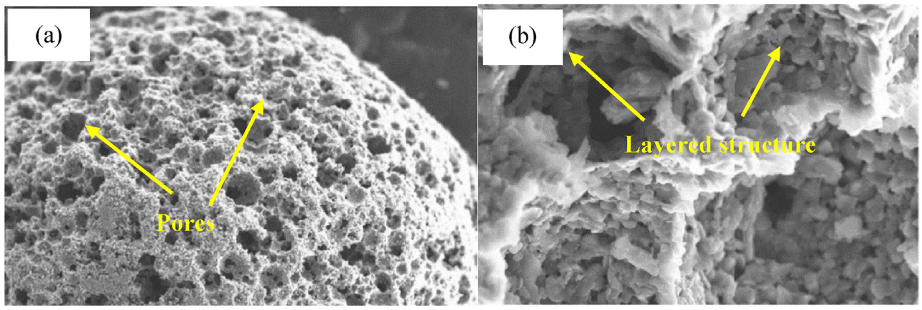

Fig. 17 – Porous geopolymeric sphere [231].

removal of heavy metals [229,230]. Potential adsorbent sites for pollutants increase after ball milling as particle size decreases, while specific area increases [222,229]. However, the main drawback of this approach is contamination, which results from the high energy condition and long milling time by the production of wear from the milling media [226].

Table 8 presents a summary on porous geopolymer adsorbents. Previously, Ge et al. [231] developed porous geopolymeric sphere using suspension and solidification method. The process begins with the preparation of slurry by dissolving NaOH in Na_2SiO_3, followed by the addition of MK and foaming agents namely 0.5% H_2O_2 and 1.5% sodium dodecyl sulphate (K12) into the alkaline solution. Then, the process continues with the preparation of geopolymeric sphere. Porous geopolymeric micro beads were prepared by continuously injecting homogeneous slurry into polyethylene glycol (PEG-600) medium under an 80 °C water bath. From Fig. 17, a porous structure of adsorbent with layered structure can be observed. This indicates that a porous geopolymeric sphere as a promising adsorbent to extract heavy metal ions was successfully synthesized. Nevertheless, the valid reason for choosing 0.5% H_2O_2 and 1.5% K12 as optimum values in the preparation of geopolymeric sphere was not declared in this work.

In the year 2016, Duan et al. [90] utilized Fe ore tailing (IOT) and FA as raw materials, which also used H_2O_2 as foaming agent to synthesize porous geopolymer for Cu^{2+} adsorption from wastewater. This work discovered that an amorphous geopolymer with total pores value of 74.6% was successfully synthesized by transforming FA and IOT into foaming geopolymer. As revealed in Fig. 18(a), the SEM image of geopolymer without addition of H_2O_2 consists of low porosity with dense structure. Whereas, after the addition of H_2O_2, high porosity structure compared to reference sample was observed, which provided more adsorption sites for adsorption as shown in Fig. 18(b). However, it would be better, if Duan et al. [90] could provide an analysis on the difference between the surface area of synthesized geopolymer and porous geopolymer in order to determine difference in the interaction between wastewater and adsorbents.

In another study, Hu et al. [232] studied the Cu^{2+} removal efficiency of activated $CaCO_3$ via ball milling. The Cu^{2+} removal was not possible only with physical adsorption from agitation process. It was found that ball milling played a vital function in activating the $CaCO_3$ sample and stimulating its reaction with copper sulphate ($CuSO_4$) as effectively as $Ca(OH)_2$. The reactivity of $CaCO_3$ with heavy metals in wastewaters could be improved by milling, which entails adding of balls to the agitation process. This is because, the principal reaction pathway for the Cu^{2+} removal is the precipitation of posnjakite, which results from the interaction between $CaCO_3$ and $CuSO_4$, which was triggered by ball milling. Other than that, wetting and dissolution behavior of $CaCO_3$ are the two main changes caused by ball impact during milling, which are dependent on the surface roughness and shape of the milled particles. Nonetheless, Hu et al. [232] study should include the adsorption experiments such as isotherms and kinetics to explore more on the adsorption mechanisms of Cu^{2+} by mechanically activated $CaCO_3$.

Similarly, Tan et al. [206] investigated the potential of prepared porous geopolymer sphere adsorbent via facile method towards adsorption of Ni^{2+} from wastewater. First of

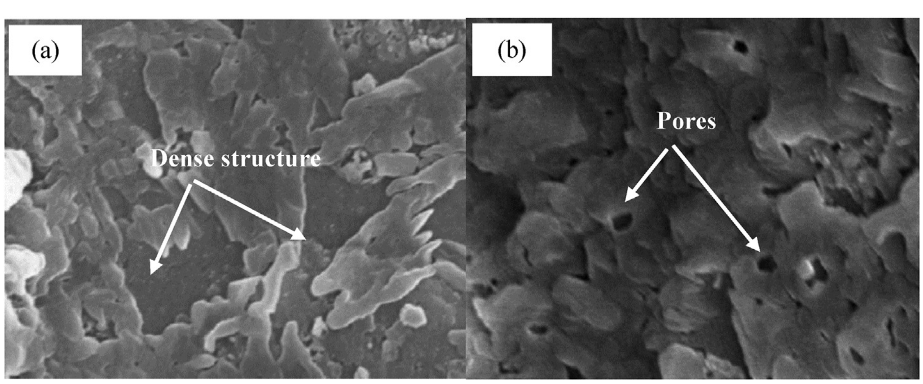

Fig. 18 – Pores structure of (a) Geopolymer and (b) Porous geopolymer [90].

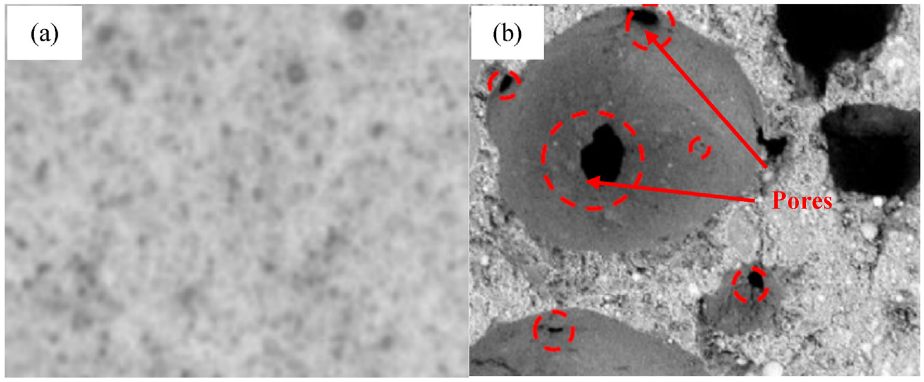

Fig. 19 – Morphology of (a) WFOA and (b) FOA [206].

all, FA and calcined clay were used as a source of aluminosilicate, mixed with alkaline activator, while H_2O_2 was used as foaming agent to develop porous structure. Upon mixing, the obtained geopolymer paste was cured for 24 h at 60 °C in an oven. Formation of compact gel structure was observed in the sample as illustrated in Fig. 19(a), prepared without foaming agent (WFOA) while formation of pores that are more visible and larger in size were discovered in the sample in Fig. 19(b) with foaming agent (FOA). However, it will be more understandable if Tan et al. [206] study could provide XRD analysis on the synthesized WFOA and FOA in order to determine the phases present before and after synthesis.

In contrast, Pachana et al. [219] examined the effect of calcination temperature on the removal of Fe^{2+} and Mn^{2+} by the porous geopolymer adsorbent by utilizing water treatment residue. Since this residue contains significant levels of SiO_2 and Al_2O_3, it may be a potential source of material for the development of geopolymers. The total pore volume was increased to 49.43 and 56.51% with increasing calcination temperature to 400 (G-400) and 600 °C (G-600) respectively due to water vaporization of sodium silicate in the geopolymer mixture. Increased in porosity with increasing calcination temperature was consistent with increased in the water adsorption. The geopolymer samples showed a dense and strong matrix after being calcined at 400 and 600 °C as shown in Fig. 20(a) and (b) respectively. The G-400 sample completely eliminated all of the Fe from the aqueous solution while about 50% of the removal of Fe^{2+} was achieved by G-600. This is because, G-600 had lower releasing capacity of OH^- than G-400 due to the dense matrix obtained. In addition, Mn^{2+} can be removed from an aqueous solution by adsorption and coprecipitation with Fe ions. The addition of alkali (OH^- ions from G-600) increased the pH of the solution, leading to an increase in Fe precipitate and the Mn removal ratio. Nevertheless, the calcination effect on the removal efficiency of Fe^{2+} and Mn^{2+} at 500 °C should be conducted to validate the best calcination temperature towards pores development and heavy metal ions removal application.

6. Summary and future works

From the review that had been done, the characteristics and potential of different aluminosilicate materials in the preparation of geopolymer based adsorbent were studied by analyzing the advantages and disadvantages of various geological origins and industrial waste materials. It can be concluded that, sludge contains significant components compared to other waste materials such as FA and slag. Thus, it can effectively adsorb heavy metal ions by the combined contribution of ion exchange, precipitation and ion complexation with heavy metals. The presence of metal oxide such and inorganic salts in sludge will increase the active site on the surface of geopolymer. On the other hand, the presence of heavy metals in sludge can be immobilized in geopolymeric matric. Utilization of sludge as aluminosilicate material in the geopolymerization process not only transform waste into assets but also produces highly effective heavy metal

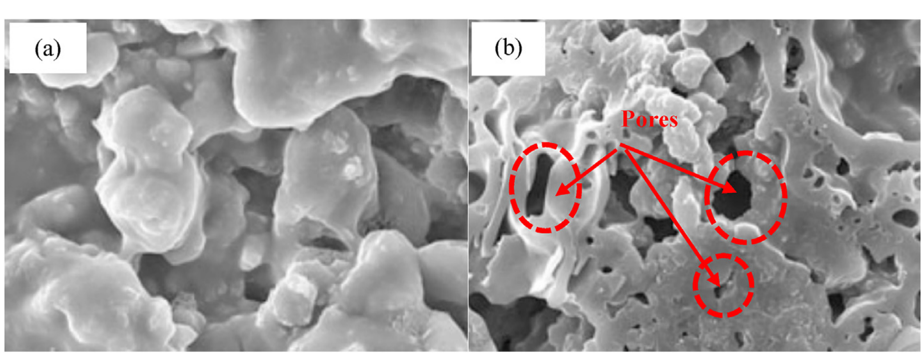

Fig. 20 – Morphology of (a) G-400 and (b) G-600 [219].

adsorbents and lowers the cost of sludge disposal. Thus, sludge based geopolymer adsorbent could deliver double benefit in waste management and wastewater treatment. In addition, the synthesis parameters such as molar concentration of alkaline activator, alkaline activator ratio, S/L and curing temperature play a significant role in the effective geopolymerization process. Thus, coming up with a proper mix design is crucial in order to precisely control each of the parameters mentioned above. Besides, this paper also reviewed several possible methods for improving the physical properties of adsorbents. Other than replica, sacrificial template and direct forming methods, sintering and ball milling are considered environmentally approaches to improve the development of pores and surface area of the adsorbents.

Based on the review that had been done, a few research gaps have been identified and several future works are proposed as listed below:

i. ZP provides important information on the electrostatic interaction between adsorbent and adsorbate while FTIR provides important information on the surface functional groups which has a significant role in the removal of heavy metals ions via adsorption. Nevertheless, previous studies on the adsorption capacity of MK based geopolymer and MK/zeolite based geopolymer did not provide the analysis results on both ZP and FTIR.
ii. Besides, EDX and XRD analysis should be conducted on the adsorbent after adsorption in order to identify the compositional elements in the adsorbed geopolymer and also to detect formation of new crystals structures through chemical reactions respectively.
iii. In addition, a study on the regeneration ability of pyrophyllite based geopolymer must identified as it is an important element in evaluating the performance of the adsorbent.
iv. Other than that, some of the researchers did not reveal some important parameters used in the geopolymerization process such as molarity of NaOH concentration, S/L ratio, and SS/SH ratio which directly influence the structure and framework of the geopolymer.
v. Other than replica, direct forming and sacrificial template, thermal and mechanical processes are physical modification methods, which improve the physical characteristics of adsorbent such as surface area, pore volume, density and solubility.
vi. From a previous study, it will be more understandable if this study could provide a schematic diagram which can illustrate the mechanisms that occur during the adsorption of Pb^{2+} and Ni^{2+}. While in another study, adsorption experiments such as isotherms and kinetics should be included to explore more on the adsorption mechanisms of Cu^{2+} by mechanically activated $CaCO_3$.
vii. However, geopolymer showed lacks the capacity to directly absorb anions and thus further studies are required for the development of geopolymer on anions adsorption efficiency.
viii. In contrast, limited studies focused on the utilization of sludge in the geopolymerization process although it has significant components that make it potential for heavy metal adsorption.

Declaration of Competing Interest

The authors declare that they have no known competing financial interests or personal relationships that could have appeared to influence the work reported in this paper.

REFERENCES

[1] Li Y, Yu H, Liu L, Yu H. Application of co-pyrolysis biochar for the adsorption and immobilization of heavy metals in contaminated environmental substrates. J Hazard Mater 2021;420:126655. https://doi.org/10.1016/j.jhazmat.2021.126655.

[2] Siong W, Ying J, Kumar PS, Mubashir M, Majeed Z, Banat F, et al. A review on conventional and novel materials towards heavy metal adsorption in wastewater treatment application. J Clean Prod 2021;296:126589. https://doi.org/10.1016/j.jclepro.2021.126589.

[3] Razzak SA, Farooque MO, Alsheikh Z, Alsheikhmohamad L, Alkuroud D, Alfayez A, et al. A comprehensive review on conventional and biological-driven heavy metals removal from industrial wastewater. Environ. Adv. 2022;7:100168. https://doi.org/10.1016/j.envadv.2022.100168.

[4] Wijeyawardana P, Nanayakkara N, Gunasekara C, Karunarathna A, Law D, Pramanik BK. Improvement of heavy metal removal from urban runoff using modified pervious concrete. Sci Total Environ 2022;815:152936. https://doi.org/10.1016/j.scitotenv.2022.152936.

[5] Kara İ, Yilmazer D, Akar ST. Metakaolin based geopolymer as an effective adsorbent for adsorption of zinc(II) and nickel(II) ions from aqueous solutions. Appl Clay Sci 2017;139:54–63. https://doi.org/10.1016/j.clay.2017.01.008.

[6] Demirbas A. Heavy metal adsorption onto agro-based waste materials: a review. J Hazard Mater 2008;157:220–9. https://doi.org/10.1016/j.jhazmat.2008.01.024.

[7] Miranda LS, Ayoko GA, Egodawatta P, Goonetilleke A. Adsorption-desorption behavior of heavy metals in aquatic environments: influence of sediment, water and metal ionic properties. J Hazard Mater 2022;421:126743. https://doi.org/10.1016/j.jhazmat.2021.126743.

[8] Li Q, Shi W, Yang Q. Polarization induced covalent bonding: a new force of heavy metal adsorption on charged particle surface. J Hazard Mater 2021;412:125168. https://doi.org/10.1016/j.jhazmat.2021.125168.

[9] Shao N, Li S, Yan F, Su Y, Liu F, Zhang Z. An all-in-one strategy for the adsorption of heavy metal ions and photodegradation of organic pollutants using steel slag-derived calcium silicate hydrate. J Hazard Mater 2020;382:121120. https://doi.org/10.1016/j.jhazmat.2019.121120.

[10] Aljaberi FY. Studies of autocatalytic electrocoagulation reactor for lead removal from simulated wastewater. J Environ Chem Eng 2018;6:6069–78. https://doi.org/10.1016/j.jece.2018.09.032.

[11] El-Ashtoukhy ESZ, Amin NK, Fouad YO, Hamad HA. Intensification of a new electrocoagulation system characterized by minimum energy consumption and maximum removal efficiency of heavy metals from simulated wastewater. Chem Eng Process Process Intensif 2020;154:108026. https://doi.org/10.1016/j.cep.2020.108026.

[12] Kanagaraj P, Nagendran A, Rana D, Matsuura T, Neelakandan S. Separation of macromolecular proteins and

rejection of toxic heavy metal ions by PEI/cSMM blend UF membranes. Int J Biol Macromol 2014;72:223–9. https://doi.org/10.1016/j.ijbiomac.2014.08.018.
[13] Igwegbe CA, Oba SN, Aniagor CO, Adeniyi AG, Ighalo JO. Adsorption of ciprofloxacin from water: a comprehensive review. J Ind Eng Chem 2021;93:57–77. https://doi.org/10.1016/j.jiec.2020.09.023.
[14] Bhattacharjee T, Islam M, Chowdhury D, Majumdar G. In-situ generated carbon dot modified filter paper for heavy metals removal in water. Environ Nanotechnol Monit Manag 2021;16:100582. https://doi.org/10.1016/j.enmm.2021.100582.
[15] Haripriyan U, Gopinath KP, Arun J. Chitosan based nano adsorbents and its types for heavy metal removal: a mini review. Mater Lett 2022;312:131670. https://doi.org/10.1016/j.matlet.2022.131670.
[16] qin Jiang M, ying Jin X, Lu XQ, liang Chen Z. Adsorption of Pb(II), Cd(II), Ni(II) and Cu(II) onto natural kaolinite clay. Desalination 2010;252:33–9. https://doi.org/10.1016/j.desal.2009.11.005.
[17] Mestre AS, Pires RA, Aroso I, Fernandes EM, Pinto ML, Reis RL, et al. Activated carbons prepared from industrial pre-treated cork: sustainable adsorbents for pharmaceutical compounds removal. Chem Eng J 2014;253:408–17. https://doi.org/10.1016/j.cej.2014.05.051.
[18] Babel S, Kurniawan TA. Low-cost adsorbents for heavy metals uptake from contaminated water: a review. J Hazard Mater 2003;97:219–43. https://doi.org/10.1016/S0304-3894(02)00263-7.
[19] Maleki A, Mohammad M, Emdadi Z, Asim N, Azizi M, Safaei J. Adsorbent materials based on a geopolymer paste for dye removal from aqueous solutions. Arab J Chem 2020;13:3017–25. https://doi.org/10.1016/j.arabjc.2018.08.011.
[20] Luhar I, Luhar S, Abdullah MMAB, Razak RA, Vizureanu P, Sandu AV, et al. A state-of-the-art review on innovative geopolymer composites designed for water and wastewater treatment. Materials 2021;14:7456. https://doi.org/10.3390/ma14237456.
[21] Zhang X, Bai C, Qiao Y, Wang X, Jia D, Li H, et al. Porous geopolymer composites: a review. Compos A Appl Sci Manuf 2021;150:106629. https://doi.org/10.1016/j.compositesa.2021.106629.
[22] He P, Zhang Y, Zhang X, Chen H. Diverse zeolites derived from a circulating fluidized bed fly ash based geopolymer for the adsorption of lead ions from wastewater. J Clean Prod 2021;312:2–11. https://doi.org/10.1016/j.jclepro.2021.127769.
[23] Novais RM, Buruberri LH, Seabra MP, Labrincha JA. Novel porous fly-ash containing geopolymer monoliths for lead adsorption from wastewaters. J Hazard Mater 2016;318:631–40. https://doi.org/10.1016/j.jhazmat.2016.07.059.
[24] Taki K, Mukherjee S, Kumar A, Kumar M. Reappraisal review on geopolymer : a new era of aluminosilicate binder for metal immobilization. Environ Nanotechnol Monit Manag 2020;14:100345. https://doi.org/10.1016/j.enmm.2020.100345.
[25] Haddaji Y, Majdoubi H, Mansouri S, Alomayri TS, Allaoui D, Manoun B, et al. Microstructure and flexural performances of glass fibers reinforced phosphate sludge based geopolymers at elevated temperatures. Case Stud Constr Mater 2022;16. https://doi.org/10.1016/j.cscm.2022.e00928.
[26] Das O, Babu K, Shanmugam V, Sykam K, Sas G, Tebyetekerwa M, et al. Natural and industrial wastes for sustainable and renewable polymer composites. Renew Sustain Energy Rev 2022;158:1–22. https://doi.org/10.1016/j.rser.2021.112054.
[27] di Chen Y, Wang R, Duan X, Wang S, qi Ren N, Ho SH. Production, properties, and catalytic applications of sludge derived biochar for environmental remediation. Water Res 2020;187:116390. https://doi.org/10.1016/j.watres.2020.116390.
[28] Niu X, Elakneswaran Y, Islam CR, Provis JL, Sato T. Adsorption behaviour of simulant radionuclide cations and anions in metakaolin-based geopolymer. J Hazard Mater 2022;429:128373. https://doi.org/10.1016/j.jhazmat.2022.128373.
[29] Wang Q, shan Li J, Poon CS. Using incinerated sewage sludge ash as a high-performance adsorbent for lead removal from aqueous solutions: performances and mechanisms. Chemosphere 2019;226:587–96. https://doi.org/10.1016/j.chemosphere.2019.03.193.
[30] Ji H, Huang W, Xing Z, Zuo J, Wang Z, Yang K. Experimental study on removing heavy metals from the municipal solid waste incineration fly ash with the modified electrokinetic remediation device. Sci Rep 2019;9:1–10. https://doi.org/10.1038/s41598-019-43844-w.
[31] Krabbenhoft DP, Sunderland EM. Global change and mercury. Science 2013;341(80):1457–8. https://doi.org/10.1126/science.1242838.
[32] Wang XY, Hao Y, Zhao HB, Guo YR, Pan QJ. 2D-layered Mg(OH)2 material adsorbing cellobiose via interfacial chemical coupling and its applications in handling toxic Cd2+ and UO22+ ions. Chemosphere 2021;279:130617. https://doi.org/10.1016/j.chemosphere.2021.130617.
[33] Spitzer J, Poolman B. The role of biomacromolecular crowding, ionic strength, and physicochemical gradients in the complexities of life's emergence. Microbiol Mol Biol Rev 2009;73:371–88. https://doi.org/10.1128/mmbr.00010-09.
[34] Grivet JP, Delort AM. NMR for microbiology: in vivo and in situ applications. Prog Nucl Magn Reson Spectrosc 2009;54:1–53. https://doi.org/10.1016/j.pnmrs.2008.02.001.
[35] Štofejová L, Fazekaš J, Fazekašová D. Analysis of heavy metal content in soil and plants in the dumping ground of magnesite mining factory jelšava-lubeník (Slovakia). Sustain Times 2021;13. https://doi.org/10.3390/su13084508.
[36] Rathnayake IVN, Megharaj M, Bolan N, Naidu R. Tolerance of heavy metals by gram positive soil bacteria. Int J Environ Eng 2010;2:191–5.
[37] Ray PZ, Shipley HJ. ChemInform abstract : inorganic nano-adsorbents for the removal of heavy metals and arsenic : a review RSC advances. RSC Adv 2015;5:29885–907. https://doi.org/10.1039/C5RA02714D.
[38] Modoi OC, Roba C, Török Z, Ozunu A. Environmental risks due to heavy metal pollution of water resulted from mining wastes in NW Romania. Environ Eng Manag J 2014;13:2325–36. https://doi.org/10.30638/eemj.2014.260.
[39] Yuan H, Ren T, Luo Q, Huang Y, Huang Y, Xu D, et al. Fluorescent wood with non-cytotoxicity for effective adsorption and sensitive detection of heavy metals. J Hazard Mater 2021;416:126166. https://doi.org/10.1016/j.jhazmat.2021.126166.
[40] Moussa DT, El-Naas MH, Nasser M, Al-Marri MJ. A comprehensive review of electrocoagulation for water treatment: potentials and challenges. J Environ Manag 2017;186:24–41. https://doi.org/10.1016/j.jenvman.2016.10.032.
[41] Kyaw HH, Myint MTZ, Al-Harthi S, Al-Abri M. Removal of heavy metal ions by capacitive deionization: effect of surface modification on ions adsorption. J Hazard Mater 2020;385. https://doi.org/10.1016/j.jhazmat.2019.121565.
[42] Fan S, Chen J, Fan C, Chen G, Liu S, Zhou H, et al. Fabrication of a CO2-responsive chitosan aerogel as an effective adsorbent for the adsorption and desorption of heavy metal ions. J Hazard Mater 2021;416:126225. https://doi.org/10.1016/j.jhazmat.2021.126225.
[43] Gupta VK, Moradi O, Tyagi I, Agarwal S, Sadegh H, Shahryari-Ghoshekandi R, et al. Study on the removal of

heavy metal ions from industry waste by carbon nanotubes: effect of the surface modification: a review. Crit Rev Environ Sci Technol 2016;46:93–118. https://doi.org/10.1080/10643389.2015.1061874.

[44] Tripathi A, Ranjan MR. Heavy metal removal from wastewater using low cost adsorbents bior emediation & biodegradation. J Bioremed Biodeg 2015;6. https://doi.org/10.4172/2155-6199.1000315.

[45] El M, Saufi H, Moutaoukil G, Alehyen S, Nematollahi B, Belmaghraoui W, et al. Application of geopolymers for treatment of water contaminated with organic and inorganic pollutants : state-of-the-art review. J Environ Chem Eng 2021;9:105095. https://doi.org/10.1016/j.jece.2021.105095.

[46] da Alves L, de Almeida Moreira BR, da Silva Viana R, Dias ES, Rinker DL, Pardo-Gimenez A, et al. Spent mushroom substrate is capable of physisorption-chemisorption of CO2. Environ Res 2022;204. https://doi.org/10.1016/j.envres.2021.111945.

[47] De Gisi S, Lofrano G, Grassi M, Notarnicola M. Characteristics and adsorption capacities of low-cost sorbents for wastewater treatment: a review. Sustain Mater Technol 2016;9:10–40. https://doi.org/10.1016/j.susmat.2016.06.002.

[48] Soliman NK, Moustafa AF. Industrial solid waste for heavy metals adsorption features and challenges ; a review. Integr Med Res 2020;9:10235–53. https://doi.org/10.1016/j.jmrt.2020.07.045.

[49] Li W, Mu B, Yang Y. Feasibility of industrial-scale treatment of dye wastewater via bio-adsorption technology. Bioresour Technol 2019;277:157–70. https://doi.org/10.1016/j.biortech.2019.01.002.

[50] Gupta VK, Tyagi I, Sadegh H, Shahryari-ghoshekandi R. Nanoparticles as adsorbent ; a positive approach for removal of noxious metal ions. A Review 2015;34:195–214. https://doi.org/10.3923/std.2015.195.214.

[51] Chai WS, Cheun JY, Kumar PS, Mubashir M, Majeed Z, Banat F, et al. A review on conventional and novel materials towards heavy metal adsorption in wastewater treatment application. J Clean Prod 2021;296:126589. https://doi.org/10.1016/j.jclepro.2021.126589.

[52] Burakov AE, Galunin EV, Burakova IV, Kucherova AE, Agarwal S, Tkachev AG, et al. Adsorption of heavy metals on conventional and nanostructured materials for wastewater treatment purposes: a review. Ecotoxicol Environ Saf 2018;148:702–12. https://doi.org/10.1016/j.ecoenv.2017.11.034.

[53] Titchou FE, Zazou H, Afanga H, El Gaayda J, Akbour RA, Hamdani M. Removal of Persistent Organic Pollutants (POPs) from water and wastewater by adsorption and electrocoagulation process. Groundw Sustain Dev 2021;13:100575. https://doi.org/10.1016/j.gsd.2021.100575.

[54] Sarkar C, Basu JK, Samanta AN. Removal of Ni2+ ion from waste water by Geopolymeric Adsorbent derived from LD Slag. J Water Proc Eng 2017;17:237–44. https://doi.org/10.1016/j.jwpe.2017.04.012.

[55] Panda L, Rath SS, Rao DS, Nayak BB, Das B, Misra PK. Thorough understanding of the kinetics and mechanism of heavy metal adsorption onto a pyrophyllite mine waste based geopolymer. J Mol Liq 2018;263:428–41. https://doi.org/10.1016/j.molliq.2018.05.016.

[56] Liu Y, Xu X, Qu B, Liu X, Yi W, Zhang H. Study on adsorption properties of modified corn cob activated carbon for mercury ion. Energies 2021;14. https://doi.org/10.3390/en14154483.

[57] Zhang Y, Zhao M, Cheng Q, Wang C, Li H, Han X, et al. Research progress of adsorption and removal of heavy metals by chitosan and its derivatives: a review. Chemosphere 2021;279. https://doi.org/10.1016/j.chemosphere.2021.130927. 130927.

[58] Badawi MA, Negm NA, Abou Kana MTH, Hefni HH, Abdel Moneem MM. Adsorption of aluminum and lead from wastewater by chitosan-tannic acid modified biopolymers: isotherms, kinetics, thermodynamics and process mechanism. Int J Biol Macromol 2017;99:465–76. https://doi.org/10.1016/j.ijbiomac.2017.03.003.

[59] Gökçe HS, Tuyan M, Nehdi ML. Alkali-activated and geopolymer materials developed using innovative manufacturing techniques: a critical review. Construct Build Mater 2021;303. https://doi.org/10.1016/j.conbuildmat.2021.124483.

[60] Yang M, Zheng Y, Li X, Yang X, Rao F, Zhong L. Durability of alkali-activated materials with different C–S–H and N-A-S-H gels in acid and alkaline environment. J Mater Res Technol 2022;16:619–30. https://doi.org/10.1016/j.jmrt.2021.12.031.

[61] Freire AL, Moura-Nickel CD, Scaratti G, De Rossi A, Araújo MH, De Noni Júnior A, et al. Geopolymers produced with fly ash and rice husk ash applied to CO_2 capture. J Clean Prod 2020;273. https://doi.org/10.1016/j.jclepro.2020.122917.

[62] Boscherini M, Miccio F, Papa E, Medri V, Landi E, Doghieri F, et al. The relevance of thermal effects during CO2 adsorption and regeneration in a geopolymer-zeolite composite: experimental and modelling insights. Chem Eng J 2021;408:127315. https://doi.org/10.1016/j.cej.2020.127315.

[63] Humberto Tommasini Vieira Ramos FJ, de Vieira Marques MF, de Oliveira Aguiar V, Jorge FE. Performance of geopolymer foams of blast furnace slag covered with poly(lactic acid) for wastewater treatment. Ceram Int 2022;48:732–43. https://doi.org/10.1016/j.ceramint.2021.09.153.

[64] Luukkonen T, Heponiemi A, Runtti H, Pesonen J, Yliniemi J, Lassi U. Application of alkali-activated materials for water and wastewater treatment: a review. Rev Environ Sci Biotechnol 2019;18:271–97. https://doi.org/10.1007/s11157-019-09494-0.

[65] Panias D, Giannopoulou I. Geopolymers : a new generation of inorganic polymeric novel materials. 2014.

[66] De Silva P, Sagoe-Crenstil K, Sirivivatnanon V. Kinetics of geopolymerization: role of Al2O3 and SiO2. Cement Concr Res 2007;37:512–8. https://doi.org/10.1016/j.cemconres.2007.01.003.

[67] Zhang YJ, Liu LC, Ni LL, Wang BL. A facile and low-cost synthesis of granulated blast furnace slag-based cementitious material coupled with Fe2O3 catalyst for treatment of dye wastewater. Appl Catal B Environ 2013:138–9. https://doi.org/10.1016/j.apcatb.2013.02.025. 9–16.

[68] Li L, Wang S, Zhu Z. Geopolymeric adsorbents from fly ash for dye removal from aqueous solution. J Colloid Interface Sci 2006;300:52–9. https://doi.org/10.1016/j.jcis.2006.03.062.

[69] Ascensão G, Seabra MP, Aguiar JB, Labrincha JA. Red mud-based geopolymers with tailored alkali diffusion properties and pH buffering ability. J Clean Prod 2017;148:23–30. https://doi.org/10.1016/j.jclepro.2017.01.150.

[70] Xie WM, Zhou FP, Bi XL, Chen DD, Li J, Sun SY, et al. Accelerated crystallization of magnetic 4A-zeolite synthesized from red mud for application in removal of mixed heavy metal ions. J Hazard Mater 2018;358:441–9. https://doi.org/10.1016/j.jhazmat.2018.07.007.

[71] Kobayashi Y, Ogata F, Nakamura T, Kawasaki N. Synthesis of novel zeolites produced from fly ash by hydrothermal treatment in alkaline solution and its evaluation as an adsorbent for heavy metal removal. J Environ Chem Eng 2020;8:3–4. https://doi.org/10.1016/j.jece.2020.103687.

[72] Koleżyński A, Król M, Żychowicz M. The structure of geopolymers—theoretical studies. J Mol Struct 2018;1163:465–71. https://doi.org/10.1016/j.molstruc.2018.03.033.

[73] Landi E, Medri V, Papa E, Dedecek J, Klein P, Benito P, et al. Alkali-bonded ceramics with hierarchical tailored porosity. Appl Clay Sci 2013;73:56–64. https://doi.org/10.1016/j.clay.2012.09.027.

[74] Mužek MN, Svilović S, Zelić J. Fly ash-based geopolymeric adsorbent for copper ion removal from wastewater. Desalination Water Treat 2014;52:2519–26. https://doi.org/10.1080/19443994.2013.792015.

[75] Rasaki SA, Bingxue Z, Guarecuco R, Thomas T, Minghui Y. Geopolymer for use in heavy metals adsorption, and advanced oxidative processes: a critical review. J Clean Prod 2019;213:42–58. https://doi.org/10.1016/j.jclepro.2018.12.145.

[76] Hu S, Zhong L, Yang X, Bai H, Ren B, Zhao Y, et al. Synthesis of rare earth tailing-based geopolymer for efficiently immobilizing heavy metals. Construct Build Mater 2020;254:119273. https://doi.org/10.1016/j.conbuildmat.2020.119273.

[77] Minelli M, Papa E, Medri V, Miccio F, Benito P, Doghieri F, et al. Characterization of novel geopolymer—zeolite composites as solid adsorbents for CO2 capture. Chem Eng J 2018;341:505–15. https://doi.org/10.1016/j.cej.2018.02.050.

[78] Freire AL, José HJ, Moreira RDFPM. Potential applications for geopolymers in carbon capture and storage. Int J Greenh Gas Control 2022;118. https://doi.org/10.1016/j.ijggc.2022.103687.

[79] Giannopoulou I, Panias D. Structure, design and applications of geopolymeric materials. In: Proceedings of the 3rd International Conference on Deformation Processing and Structure of Materials; 2007. p. 8. https://www.researchgate.net/publication/234107877.

[80] Qin Y, Chen X, Li B, Guo Y, Niu Z, Xia T, et al. Study on the mechanical properties and microstructure of chitosan reinforced metakaolin-based geopolymer. Construct Build Mater 2021;271. https://doi.org/10.1016/j.conbuildmat.2020.121522.

[81] Bagci C, Kutyla GP, Kriven WM. Fully reacted high strength geopolymer made with diatomite as a fumed silica alternative. Ceram Int 2017;43:14784–90. https://doi.org/10.1016/j.ceramint.2017.07.222.

[82] El Alouani M, Alehyen S, El Achouri M, Taibi M. Removal of cationic dye—methylene blue- from aqueous solution by adsorption on fly ash-based geopolymer. J Mater Environ Sci 2018;9:32–46. https://doi.org/10.26872/jmes.2018.9.1.5.

[83] Liang K, Wang XQ, Chow CL, Lau D. A review of geopolymer and its adsorption capacity with molecular insights: a promising adsorbent of heavy metal ions. J Environ Manag 2022;322:116066. https://doi.org/10.1016/j.jenvman.2022.116066.

[84] El-Eswed BI, Aldagag OM, Khalili FI. Efficiency and mechanism of stabilization/solidification of Pb(II), Cd(II), Cu(II), Th(IV) and U(VI) in metakaolin based geopolymers. Appl Clay Sci 2017;140:148–56. https://doi.org/10.1016/j.clay.2017.02.003.

[85] Maleki A, Hajizadeh Z, Shari V, Emdadi Z. A green, porous and eco-friendly magnetic geopolymer adsorbent for heavy metals removal from aqueous solutions. Journal of Cleaner Production 2019;vol. 215:1233–45. https://doi.org/10.1016/j.jclepro.2019.01.084.

[86] El-eswed BI. Journal of Environmental Chemical Engineering Chemical evaluation of immobilization of wastes containing Pb , Cd , Cu and Zn in alkali-activated materials : a critical review. J Environ Chem Eng 2020;8:104194. https://doi.org/10.1016/j.jece.2020.104194.

[87] Ji Z, Pei Y. Bibliographic and visualized analysis of geopolymer research and its application in heavy metal immobilization: a review. J Environ Manag 2019;231:256–67. https://doi.org/10.1016/j.jenvman.2018.10.041.

[88] Chen X, Guo Y, Ding S, Zhang HY, Xia FY, Wang J, et al. Utilization of red mud in geopolymer-based pervious concrete with function of adsorption of heavy metal ions. J Clean Prod 2019. https://doi.org/10.1016/j.jclepro.2018.09.263.

[89] Siyal AA, Shamsuddin MR, Khan MI, Rabat NE, Zulfiqar M, Man Z, et al. A review on geopolymers as emerging materials for the adsorption of heavy metals and dyes. J Environ Manag 2018;224:327–39. https://doi.org/10.1016/j.jenvman.2018.07.046.

[90] Duan P, Yan C, Zhou W, Ren D. Development of fly ash and iron ore tailing based porous geopolymer for removal of Cu(II) from wastewater. Ceram Int 2016;42:13507–18. https://doi.org/10.1016/j.ceramint.2016.05.143.

[91] Chen S, Ruan S, Zeng Q, Liu Y, Zhang M, Tian Y, et al. Pore structure of geopolymer materials and its correlations to engineering properties: a review. Construct Build Mater 2022;328:127064. https://doi.org/10.1016/j.conbuildmat.2022.127064.

[92] Yu X, Chen L, Komarneni S, Hui C. Fly ash-based geopolymer : clean production , properties and applications. J Clean Prod 2016;125:253–67. https://doi.org/10.1016/j.jclepro.2016.03.019.

[93] Wang H, Li H, Yan F. Synthesis and mechanical properties of metakaolinite-based geopolymer. Colloids Surf A Physicochem Eng Asp 2005;268:1–6. https://doi.org/10.1016/j.colsurfa.2005.01.016.

[94] Taki K, Mukherjee S, Patel AK, Kumar M. Reappraisal review on geopolymer: a new era of aluminosilicate binder for metal immobilization. Environ Nanotechnol Monit Manag 2020;14:100345. https://doi.org/10.1016/j.enmm.2020.100345.

[95] Ren B, Zhao Y, Bai H, Kang S, Zhang T, Song S. Eco-friendly geopolymer prepared from solid wastes: a critical review. Chemosphere 2021;267:128900. https://doi.org/10.1016/j.chemosphere.2020.128900.

[96] Mills J, Mondal P, Wagner N. Structure-property relationships and state behavior of alkali-activated aluminosilicate gels. Cement Concr Res 2022;151:106618. https://doi.org/10.1016/j.cemconres.2021.106618.

[97] Yan S, Zhang F, Wang L, Rong Y, He P, Jia D, et al. A green and low-cost hollow gangue microsphere/geopolymer adsorbent for the effective removal of heavy metals from wastewaters. J Environ Manag 2019;246:174–83. https://doi.org/10.1016/j.jenvman.2019.05.120.

[98] Acisli O, Acar I, Khataee A. Preparation of a fly ash-based geopolymer for removal of a cationic dye: isothermal, kinetic and thermodynamic studies. J Ind Eng Chem 2020;83:53–63. https://doi.org/10.1016/j.jiec.2019.11.012.

[99] Alshaaer M, Zaharaki D, Komnitsas K. Microstructural characteristics and adsorption potential of a zeolitic tuff–metakaolin geopolymer. Desalination Water Treat 2015;56:338–45. https://doi.org/10.1080/19443994.2014.938306.

[100] Wang C, Li J, Wang L, Sun X, Huang J. Adsorption of dye from wastewater by zeolites synthesized from fly ash: kinetic and equilibrium studies. Chin J Chem Eng 2009;17:513–21. https://doi.org/10.1016/S1004-9541(08)60239-6.

[101] Li J, Li J, Wei H, Yang X, Benoit G, Jiao X. Alkaline-thermal activated electrolytic manganese residue-based geopolymers for efficient immobilization of heavy metals. Construct Build Mater 2021;298:123853. https://doi.org/10.1016/j.conbuildmat.2021.123853.

[102] Zhang Q, Cao X, Sun S, Yang W, Fang L, Ma R, et al. Lead zinc slag-based geopolymer: demonstration of heavy metal solidification mechanism from the new perspectives of

electronegativity and ion potential. Environ Pollut 2022;293:118509. https://doi.org/10.1016/j.envpol.2021.118509.

[103] Su Q, Li S, Chen M, Cui X. Highly efficient Cd(II) removal using macromolecular dithiocarbamate/slag-based geopolymer composite microspheres (SGM-MDTC). Separ Purif Technol 2022;286. https://doi.org/10.1016/j.seppur.2021.120395. 120395.

[104] Yan S, Ren X, Zhang F, Huang K, Feng X, Xing P. Comparative study of Pb2+, Ni2+, and methylene blue adsorption on spherical waste solid-based geopolymer adsorbents enhanced with carbon nanotubes. Separ Purif Technol 2022;284:120234. https://doi.org/10.1016/j.seppur.2021.120234.

[105] Chin JF, Heng ZW, Teoh HC, Chong WC, Pang YL. Recent development of magnetic biochar crosslinked chitosan on heavy metal removal from wastewater—modification, application and mechanism. Chemosphere 2022;291:133035. https://doi.org/10.1016/j.chemosphere.2021.133035.

[106] Blackford MG, Hanna JV, Pike KJ, Vance ER, Perera DS. Transmission electron microscopy and nuclear magnetic resonance studies of geopolymers for radioactive waste immobilization. J Am Ceram Soc 2007;90:1193–9. https://doi.org/10.1111/j.1551-2916.2007.01532.x.

[107] Van Jaarsveld JGS, Van Deventer JSJ. Effect of metal contaminants on the formation and properties of waste-based geopolymers. Cement Concr Res 1999;29:1189–200. https://doi.org/10.1016/S0008-8846(99)00032-0.

[108] Inyang MI, Gao B, Yao Y, Xue Y, Zimmerman A, Mosa A, et al. A review of biochar as a low-cost adsorbent for aqueous heavy metal removal. Crit Rev Environ Sci Technol 2016;46:406–33. https://doi.org/10.1080/10643389.2015.1096880.

[109] Long WJ, Ye TH, Xing F, Khayat KH. Decalcification effect on stabilization/solidification performance of Pb-containing geopolymers. Cem Concr Compos 2020;114:103803. https://doi.org/10.1016/j.cemconcomp.2020.103803.

[110] Wang S, Zhong S, Zheng X, Xiao D, Zheng L, Yang Y, et al. Calcite modification of agricultural waste biochar highly improves the adsorption of Cu(II) from aqueous solutions. J Environ Chem Eng 2021;9:106215. https://doi.org/10.1016/j.jece.2021.106215.

[111] Yu Z, Song W, Li J, Li Q. Improved simultaneous adsorption of Cu(II) and Cr(VI) of organic modified metakaolin-based geopolymer. Arab J Chem 2020;13:4811–23. https://doi.org/10.1016/j.arabjc.2020.01.001.

[112] Ma X, Xu D, Li Y, Ou Z, Howard A. Synthesis of a new porous geopolymer from foundry dust to remove Pb2+ and Ni2+ from aqueous solutions. J Clean Prod 2022;349:131488. https://doi.org/10.1016/j.jclepro.2022.131488.

[113] López FJ, Sugita S, Tagaya M, Kobayashi T. Metakaolin-based geopolymers for targeted adsorbents to heavy metal ion separation. J Mater Sci Chem Eng 2014;2:16–27. https://doi.org/10.4236/msce.2014.27002.

[114] Lee S, Van Riessen A, Chon C, Kang N, Jou H, Kim Y. Impact of activator type on the immobilisation of lead in fly ash-based geopolymer. Elsevier B.V; 2015. https://doi.org/10.1016/j.jhazmat.2015.11.023.

[115] Qin L, Zeng G, Lai C, Huang D, Xu P, Zhang C, et al. " Gold rush " in modern science : fabrication strategies and typical advanced applications of gold nanoparticles in sensing. Coord Chem Rev 2018;359:1–31. https://doi.org/10.1016/j.ccr.2018.01.006.

[116] Al-Zboon K, Al-Harahsheh MS, Hani FB. Fly ash-based geopolymer for Pb removal from aqueous solution. J Hazard Mater 2011;188:414–21. https://doi.org/10.1016/j.jhazmat.2011.01.133.

[117] Criado M, Vicent M, García-Ten FJ. Reactivation of alkali-activated materials made up of fly ashes from a coal power plant. Clean Mater 2022;3:100043. https://doi.org/10.1016/j.clema.2022.100043.

[118] Darmayanti L, Kadja GTM, Notodarmojo S, Damanhuri E, Mukti RR. Structural alteration within fly ash-based geopolymers governing the adsorption of Cu2+ from aqueous environment: effect of alkali activation. J Hazard Mater 2019;377:305–14. https://doi.org/10.1016/j.jhazmat.2019.05.086.

[119] El Alouani M, Alehyen S, El Achouri M, Taibi M. Preparation, characterization, and application of metakaolin-based geopolymer for removal of methylene blue from aqueous solution. J Chem 2019.

[120] Gasca-Tirado JR, Manzano-Ramírez A, RiveraMuñoz EM, Velázquez-Castillo R, Apátiga-Castro M, Nava R, et al. Ion exchange in geopolymers. New Trends Ion Exch. Stud. 2018. https://doi.org/10.5772/intechopen.80970.

[121] Ramasamy S, Mustafa M, Bakri A, Huang Y. Correlation between hardness and water absorption properties of Saudi kaolin and white clay geopolymer coating. In: AIP conference proceedings; 2017, 020224. https://doi.org/10.1063/1.5002418.

[122] El Alouani M, Saufi H, Moutaoukil G, Alehyen S, Nematollahi B, Belmaghraoui W, et al. Application of geopolymers for treatment of water contaminated with organic and inorganic pollutants: state-of-the-art review. J Environ Chem Eng 2021;9:105095. https://doi.org/10.1016/j.jece.2021.105095.

[123] Heah CY, Kamarudin H, Al AMM, Bnhussain M, Luqman M, Nizar IK, et al. Study on solids-to-liquid and alkaline activator ratios on kaolin-based Geopolymers. Constr Build Mater 2012;35:912–22. https://doi.org/10.1016/j.conbuildmat.2012.04.102.

[124] Nandi BK, Goswami A, Purkait MK. Adsorption characteristics of brilliant green dye on kaolin. J Hazard Mater 2009;161:387–95. https://doi.org/10.1016/j.jhazmat.2008.03.110.

[125] Derouiche R, Baklouti S. Phosphoric acid based geopolymerization: effect of the mechanochemical and the thermal activation of the kaolin. Ceram Int 2021;47:13446–56. https://doi.org/10.1016/j.ceramint.2021.01.203.

[126] Rożek P, Król M, Mozgawa W. Geopolymer-zeolite composites: a review. J Clean Prod 2019;230:557–79. https://doi.org/10.1016/j.jclepro.2019.05.152.

[127] Perumal P, Hasnain A, Luukkonen T, Kinnunen P, Illikainen M. Role of surfactants on the synthesis of impure kaolin-based alkali-activated, low-temperature porous ceramics. Open Ceram 2021;6:100097. https://doi.org/10.1016/j.oceram.2021.100097.

[128] Cheng TW, Lee ML, Ko MS, Ueng TH, Yang SF. Applied Clay Science the heavy metal adsorption characteristics on metakaolin-based geopolymer. Applied Clay Science 2012;56:90–6. https://doi.org/10.1016/j.clay.2011.11.027.

[129] Habert G, D'Espinose De Lacaillerie JB, Roussel N. An environmental evaluation of geopolymer based concrete production: reviewing current research trends. J Clean Prod 2011;19:1229–38. https://doi.org/10.1016/j.jclepro.2011.03.012.

[130] Rashad AM. Metakaolin as cementitious material: history, scours, production and composition-A comprehensive overview. Construct Build Mater 2013;41:303–18. https://doi.org/10.1016/j.conbuildmat.2012.12.001.

[131] Poon CS, Lam L, Kou SC, Wong YL, Wong R. Rate of pozzolanic reaction of metakaolin in high-performance cement pastes. Cement Concr Res 2001;31:1301–6. https://doi.org/10.1016/S0008-8846(01)00581-6.

[132] Rashad AM. Alkali-activated metakaolin: a short guide for civil Engineer-An overview. Construct Build Mater 2013;41:751–65. https://doi.org/10.1016/j.conbuildmat.2012.12.030.
[133] Andrejkovičová S, Sudagar A, Rocha J, Patinha C, Hajjaji W, Da Silva EF, et al. The effect of natural zeolite on microstructure, mechanical and heavy metals adsorption properties of metakaolin based geopolymers. Appl Clay Sci 2016;126:141–52. https://doi.org/10.1016/j.clay.2016.03.009.
[134] Mulugeta D, Liao Z, Berardi U, Doan H. Salient parameters affecting the performance of foamed geopolymers as sustainable insulating materials. Construct Build Mater 2021;313:125400. https://doi.org/10.1016/j.conbuildmat.2021.125400.
[135] Marroccoli M, Ibris N, Telesca A, Tregambi C, Solimene R, Di Lauro F, et al. Dolomite-based binders manufactured using concentrated solar energy in a fluidised bed reactor. Sol Energy 2022;232:471–82. https://doi.org/10.1016/j.solener.2022.01.007.
[136] Algoufi YT, Kabir G, Hameed BH. Synthesis of glycerol carbonate from biodiesel by-product glycerol over calcined dolomite. J Taiwan Inst Chem Eng 2017;70:179–87. https://doi.org/10.1016/j.jtice.2016.10.039.
[137] Bessa LP, Terra NM, Cardoso VL, Reis MHM. Macro-porous dolomite hollow fibers sintered at different temperatures toward widened applications. Ceram Int 2017;43:16283–91. https://doi.org/10.1016/j.ceramint.2017.08.214.
[138] Ibrahim AB, Abass MR, El-Masry EH, Abou-Mesalam MM. Gamma radiation-induced polymerization of polyacrylic acid-dolomite composite and applications for removal of cesium, cobalt, and zirconium from aqueous solutions. Appl Radiat Isot 2021;178:109956. https://doi.org/10.1016/j.apradiso.2021.109956.
[139] Saranya P, Nagarajan P, Shashikala AP. Behaviour of GGBS-dolomite geopolymer concrete short column under axial loading. J Build Eng 2020;30:101232. https://doi.org/10.1016/j.jobe.2020.101232.
[140] Ouda AS, Gharieb M. Development the properties of brick geopolymer pastes using concrete waste incorporating dolomite aggregate. J Build Eng 2020;27:100919. https://doi.org/10.1016/j.jobe.2019.100919.
[141] Omar K, Vilc J. Removal of toxic metals from petroleum produced water by dolomite filtration. J Water Process Eng 2022;47. https://doi.org/10.1016/j.jwpe.2022.102682.
[142] Kamarzamann FF, Abdullah MMAB, Abd Rahim SZ, Abdul Kadir A, Jamil NH, Wan Ibrahim WM, et al. Hydroxyapatite/Dolomite alkaline activated material reaction in the formation of low temperature sintered ceramic as adsorbent materials. Construct Build Mater 2022;349:128603. https://doi.org/10.1016/j.conbuildmat.2022.128603.
[143] ASTM C618-22. Standard specification for coal fly ash and raw or calcined natural pozzolan for use in concrete. West Conshohocken, PA: ASTM International; 2022.
[144] BS EN 197-5. Cement-portland-composite cement CEM II/C-M and composite cement CEM VI. British Standard Instituition BSI; 2021.
[145] Zhang LV, Marani A, Nehdi ML. Chemistry-informed machine learning prediction of compressive strength for alkali-activated materials. Constr Build Mater 2022;316:126103. https://doi.org/10.1016/j.conbuildmat.2021.126103.
[146] British Standard Institution BSI. Methods of testing composition, specifications and conformity criteria for common cements. 2011.
[147] Criado M, Palomo A, Fernández-Jiménez A. Alkali activation of fly ashes. Part 1: effect of curing conditions on the carbonation of the reaction products. Fuel 2005;84:2048–54. https://doi.org/10.1016/j.fuel.2005.03.030.
[148] Canımkurbey B. Investigation dielectric and morphological properties of fly ash collected from thermal power plant. Asia Pac J Chem Eng 2020;15:1–8. https://doi.org/10.1002/apj.2437.
[149] Javadian H, Ghorbani F, allah Tayebi H, Asl SMH. Study of the adsorption of Cd (II) from aqueous solution using zeolite-based geopolymer, synthesized from coal fly ash; kinetic, isotherm and thermodynamic studies. Arab J Chem 2015;8:837–49. https://doi.org/10.1016/j.arabjc.2013.02.018.
[150] Li X, Li J, Bai C, Zheng T, Yang K, Zhang X, et al. Preparation of porous slag-based geopolymer spheres by direct template route for pH buffering applications. Mater Lett 2022;328:133100. https://doi.org/10.1016/j.matlet.2022.133100.
[151] Jamil NH, Al Bakri Abdullah MM, Pa FC, Mohamad H, Ibrahim WMAW, Chaiprapa J. Influences of SiO2, Al2O3, CaO and MgO in phase transformation of sintered kaolin-ground granulated blast furnace slag geopolymer. J Mater Res Technol 2020;9. https://doi.org/10.1016/j.jmrt.2020.10.045. 14922–14932.
[152] Amran YHM, Alyousef R, Alabduljabbar H. Clean production and properties of geopolymer concrete ; a review. J Clean Prod 2020;251:119679. https://doi.org/10.1016/j.jclepro.2019.119679.
[153] Wen N, Zhao Y, Yu Z, Liu M. A sludge and modi fi ed rice husk ash-based geopolymer : synthesis and characterization analysis. J Clean Prod 2019;226:805–14. https://doi.org/10.1016/j.jclepro.2019.04.045.
[154] Kozai N, Sato J, Osugi T, Shimoyama I, Sekine Y, Sakamoto F, et al. Sewage sludge ash contaminated with radiocesium: solidification with alkaline-reacted metakaolinite (geopolymer) and Portland cement. J Hazard Mater 2021;416:125965. https://doi.org/10.1016/j.jhazmat.2021.125965.
[155] Petrus HTBM, Fairuz FI, Sa'dan N, Olvianas M, Astuti W, Jenie SNA, et al. Green geopolymer cement with dry activator from geothermal sludge and sodium hydroxide. J Clean Prod 2021;293:126143. https://doi.org/10.1016/j.jclepro.2021.126143.
[156] Jin M, Wang Z, Lian F, Zhao P. Freeze-thaw resistance and seawater corrosion resistance of optimized tannery sludge/metakaolin-based geopolymer. Construct Build Mater 2020;265:120730. https://doi.org/10.1016/j.conbuildmat.2020.120730.
[157] Taki K, Raval NP, Kumar M. Utilization of sewage sludge derived magnetized geopolymeric adsorbent for geogenic arsenic removal: a sustainable groundwater in-situ treatment perspective. J Clean Prod 2021;295:126466. https://doi.org/10.1016/j.jclepro.2021.126466.
[158] shan Li J, Tsang DCW, ming Wang Q, Fang L, Xue Q, Poon CS. Fate of metals before and after chemical extraction of incinerated sewage sludge ash. Chemosphere 2017;186:350–9. https://doi.org/10.1016/j.chemosphere.2017.08.012.
[159] Guo B, Pan D, Liu B, Volinsky AA, Fincan M, Du J, et al. Immobilization mechanism of Pb in fly ash-based geopolymer. Constr Build Mater 2017;134:123–30. https://doi.org/10.1016/j.conbuildmat.2016.12.139.
[160] Santos GZB, Melo JA, Pinheiro M, Manzato L. Synthesis of water treatment sludge ash-based geopolymers in an Amazonian context. J Environ Manag 2019;249:109328. https://doi.org/10.1016/j.jenvman.2019.109328.
[161] Messina F, Ferone C, Molino A, Roviello G, Colangelo F, Molino B, et al. Synergistic recycling of calcined clayey sediments and water potabilization sludge as geopolymer precursors : upscaling from binders to precast paving cement-free bricks. Constr Build Mater 2017;133:14–26. https://doi.org/10.1016/j.conbuildmat.2016.12.039.

[162] Dassanayake KB, Jayasinghe GY, Surapaneni A, Hetherington C. A review on alum sludge reuse with special reference to agricultural applications and future challenges. Waste Manag 2015;38:321–35. https://doi.org/10.1016/j.wasman.2014.11.025.

[163] Xiao X, Tan JK, Yuan JK, Fang P, Huang JH, Tang ZJ, et al. Dual role of O2 concentration on the reducing gases produced and NO reduction during sewage sludge combustion in pilot scale cement precalciner. Waste Manag 2022;137:100–9. https://doi.org/10.1016/j.wasman.2021.10.034.

[164] Chang Z, Long G, Xie Y, Zhou JL. Pozzolanic reactivity of aluminum-rich sewage sludge ash: influence of calcination process and effect of calcination products on cement hydration. Constr Build Mater 2022;318:126096. https://doi.org/10.1016/j.conbuildmat.2021.126096.

[165] Waijarean N, Asavapisit S, Sombatsompop K. Strength and microstructure of water treatment residue-based geopolymers containing heavy metals. Constr Build Mater 2014;50:486–91. https://doi.org/10.1016/j.conbuildmat.2013.08.047.

[166] Guo X, Shi H, Dick W. Use of heat-treated water treatment residuals in fly ash-based geopolymers. J Am Ceram Soc 2010;93:272–8. https://doi.org/10.1111/j.1551-2916.2009.03331.x.

[167] Tchakouté HK, Rüscher CH, Kong S, Kamseu E, Leonelli C. Thermal behavior of metakaolin-based geopolymer cements using sodium waterglass from rice husk ash and waste glass as alternative activators. Waste Biomass Valorization 2017;8:573–84. https://doi.org/10.1007/s12649-016-9653-7.

[168] Saeed KA, Kassim KA, Nur H. Physicochemical characterization of cement treated kaolin clay. Gradjevinar 2014;66:513–21. https://doi.org/10.14256/JCE.976.2013.

[169] Sarkar M, Dana K. Partial replacement of metakaolin with red ceramic waste in geopolymer. 2020.

[170] Piol MN, Dickerman C, Ardanza MP, Saralegui A, Boeykens SP. Simultaneous removal of chromate and phosphate using different operational combinations for their adsorption on dolomite and banana peel. J Environ Manag 2021;288:112463. https://doi.org/10.1016/j.jenvman.2021.112463.

[171] Hu H, Zhang Q, Li X, Wu L, Liu Y. Efficient heterogeneous precipitation and separation of iron in copper-containing solution using dolomite. Separ Purif Technol 2020;248:117021. https://doi.org/10.1016/j.seppur.2020.117021.

[172] Al Bakri Abdullah MM, Hussin K, Bnhussain M, Ismail KN, Yahya Z, Razak RA. Fly ash-based geopolymer lightweight concrete using foaming agent. Int J Mol Sci 2012;13:7186–98. https://doi.org/10.3390/ijms13067186.

[173] Gopinath A, Divyapriya G, Srivastava V, Laiju AR, V Nidheesh P, Kumar MS. Conversion of sewage sludge into biochar : a potential resource in water and wastewater treatment. Environ Res 2021;194:110656. https://doi.org/10.1016/j.envres.2020.110656.

[174] Hawari AH, Mulligan CN. Effect of the presence of lead on the biosorption of copper, cadmium and nickel by anaerobic biomass. Process Biochem 2007;42:1546–52. https://doi.org/10.1016/j.procbio.2007.08.009.

[175] Wang C, Yang Z, Song W, Zhong Y, Sun M, Gan T, et al. Quantifying gel properties of industrial waste-based geopolymers and their application in Pb2+ and Cu2+ removal. J Clean Prod 2021;315:128203. https://doi.org/10.1016/j.jclepro.2021.128203.

[176] Samantasinghar S, Singh SP. Effect of synthesis parameters on compressive strength of fly ash-slag blended geopolymer. Construct Build Mater 2018;170:225–34. https://doi.org/10.1016/j.conbuildmat.2018.03.026.

[177] Degefu DM, Liao Z, Berardi U, Labbé G. The effect of activator ratio on the thermal and hygric properties of aerated geopolymers. J Build Eng 2022;45:103414. https://doi.org/10.1016/j.jobe.2021.103414.

[178] Farhan KZ, Johari MAM, Demirboğa R. Assessment of important parameters involved in the synthesis of geopolymer composites: a review. Constr Build Mater 2020;264. https://doi.org/10.1016/j.conbuildmat.2020.120276.

[179] Somna K, Jaturapitakkul C, Kajitvichyanukul P, Chindaprasirt P. NaOH-activated ground fly ash geopolymer cured at ambient temperature. Fuel 2011;90:2118–24. https://doi.org/10.1016/j.fuel.2011.01.018.

[180] Pangdaeng S, Sata V, Aguiar JB, Pacheco-Torgal F, Chindaprasirt P. Apatite formation on calcined kaolin-white Portland cement geopolymer. Mater Sci Eng C 2015;51:1–6. https://doi.org/10.1016/j.msec.2015.02.039.

[181] Yunsheng Z, Wei S, Zongjin L. Applied Clay Science Composition design and microstructural characterization of calcined kaolin-based geopolymer cement. Appl Clay Sci 2010;47:271–5. https://doi.org/10.1016/j.clay.2009.11.002.

[182] Fernández-Jiménez A, Palomo A. Composition and microstructure of alkali activated fly ash binder: effect of the activator. Cement Concr Res 2005;35:1984–92. https://doi.org/10.1016/j.cemconres.2005.03.003.

[183] Xu H, Van Deventer JSJ. The effect of alkali metals on the formation of geopolymeric gels from alkali-feldspars. Colloids Surf A Physicochem Eng Asp 2003;216:27–44. https://doi.org/10.1016/S0927-7757(02)00499-5.

[184] Poloju KK, Srinivasu K. Impact of GGBS and strength ratio on mechanical properties of geopolymer concrete under ambient curing and oven curing. Mater Today Proc 2020;42:962–8. https://doi.org/10.1016/j.matpr.2020.11.934.

[185] Görhan G, Kürklü G. The influence of the NaOH solution on the properties of the fly ash-based geopolymer mortar cured at different temperatures. Compos B Eng 2014;58:371–7. https://doi.org/10.1016/j.compositesb.2013.10.082.

[186] Chindaprasirt P, Jaturapitakkul C, Chalee W, Rattanasak U. Comparative study on the characteristics of fly ash and bottom ash geopolymers. Waste Manag 2009;29:539–43. https://doi.org/10.1016/j.wasman.2008.06.023.

[187] Muraleedharan M, Nadir Y. Factors affecting the mechanical properties and microstructure of geopolymers from red mud and granite waste powder: a review. Ceram Int 2021;47:13257–79. https://doi.org/10.1016/j.ceramint.2021.02.009.

[188] Gharzouni A, Joussein E, Samet B, Baklouti S, Rossignol S. Effect of the reactivity of alkaline solution and metakaolin on geopolymer formation. J Non-Cryst Solids 2015;410:127–34. https://doi.org/10.1016/j.jnoncrysol.2014.12.021.

[189] Liew YM, Heah CY, Mohd Mustafa AB, Kamarudin H. Structure and properties of clay-based geopolymer cements: a review. Prog Mater Sci 2016;83:595–629. https://doi.org/10.1016/j.pmatsci.2016.08.002.

[190] Palmero P, Formia A, Antonaci P, Brini S, Tulliani JM. Geopolymer technology for application-oriented dense and lightened materials. Elaboration and characterization. Ceram Int 2015;41:12967–79. https://doi.org/10.1016/j.ceramint.2015.06.140.

[191] Alonso S, Palomo A. Alkaline activation of metakaolin and calcium hydroxide mixtures: influence of temperature, activator concentration and solids ratio. Mater Lett 2001;47:55–62. https://doi.org/10.1016/S0167-577X(00)00212-3.

[192] Luo Y, Meng J, Wang D, Jiao L, Xue G. Experimental study on mechanical properties and microstructure of metakaolin based geopolymer stabilized silty clay. Constr Build Mater 2022;316:125662. https://doi.org/10.1016/j.conbuildmat.2021.125662.
[193] Cheng H, Lin KL, Cui R, Hwang CL, Cheng TW, Chang YM. Effect of solid-to-liquid ratios on the properties of waste catalyst-metakaolin based geopolymers. Constr Build Mater 2015;88:74–83. https://doi.org/10.1016/j.conbuildmat.2015.01.005.
[194] Bowen F, Jiesheng L, Jing W, Yaohua C, Tongtong Z. Case Studies in Construction Materials Investigation on the impact of different activator to solid ratio on properties and micro-structure of metakaolin geopolymer. Case Stud Constr Mater 2022;16:e01127. https://doi.org/10.1016/j.cscm.2022.e01127.
[195] Sagoe-Crentsil K, Weng L. Dissolution processes, hydrolysis and condensation reactions during geopolymer synthesis: Part II. High Si/Al ratio systems. J Mater Sci 2007;42:3007–14. https://doi.org/10.1007/s10853-006-0818-9.
[196] Weng L, Sagoe-Crentsil K. Dissolution processes, hydrolysis and condensation reactions during geopolymer synthesis: Part I-Low Si/Al ratio systems. J Mater Sci 2007;42:2997–3006. https://doi.org/10.1007/s10853-006-0820-2.
[197] He J, Jie Y, Zhang J, Yu Y, Zhang G. Cement & Concrete Composites Synthesis and characterization of red mud and rice husk ash-based geopolymer composites. Cem Concr Compos 2013;37:108–18. https://doi.org/10.1016/j.cemconcomp.2012.11.010.
[198] Zhang B, Yuan P, Guo H, Deng L, Li Y, Li L, et al. Effect of curing conditions on the microstructure and mechanical performance of geopolymers derived from nanosized tubular halloysite. 2020. https://doi.org/10.1016/j.conbuildmat.2020.121186.
[199] Sajan P, Jiang T, Lau C, Tan G, Ng K. Combined effect of curing temperature, curing period and alkaline concentration on the mechanical properties of fly ash-based geopolymer. Clean Mater 2021;1:100002. https://doi.org/10.1016/j.clema.2021.100002.
[200] Kara I, Tunc D, Sayin F, Akar ST. Study on the performance of metakaolin based geopolymer for Mn(II) and Co(II) removal. Appl Clay Sci 2018;161:184–93. https://doi.org/10.1016/j.clay.2018.04.027.
[201] Ghani U, Hussain S, Imtiaz M. Laterite clay-based geopolymer as a potential adsorbent for the heavy metals removal from aqueous solutions. J Saudi Chem Soc 2020;24:874–84. https://doi.org/10.1016/j.jscs.2020.09.004.
[202] Lan T, Guo S, Li X, Guo J, Bai T, Zhao Q, et al. Mixed precursor geopolymer synthesis for removal of Pb(II) and Cd(II). Mater Lett 2020;274:127977. https://doi.org/10.1016/j.matlet.2020.127977.
[203] Wei E, Wang K, Muhammad Y, Chen S, Dong D, Wei Y, et al. Preparation and conversion mechanism of different geopolymer-based zeolite microspheres and their adsorption properties for Pb 2 +. Separ Purif Technol 2022;282:119971. https://doi.org/10.1016/j.seppur.2021.119971.
[204] Sanguanpak S, Wannagon A, Saengam C, Chiemchaisri W, Chiemchaisri C. Porous metakaolin-based geopolymer granules for removal of ammonium in aqueous solution and anaerobically pretreated piggery wastewater. J Clean Prod 2021;297:126643. https://doi.org/10.1016/j.jclepro.2021.126643.
[205] Studart AR, Gonzenbach UT, Tervoort E, Gauckler LJ. Processing routes to macroporous ceramics: a review. J Am Ceram Soc 2006;89:1771–89. https://doi.org/10.1111/j.1551-2916.2006.01044.x.
[206] Tan TH, Mo KH, Lai SH, Ling TC. Synthesis of porous geopolymer sphere for Ni(II) removal. Ceram Int 2021;47:29055–63. https://doi.org/10.1016/j.ceramint.2021.06.268.
[207] Thommes M, Kaneko K, Neimark AV, Olivier JP, Rodriguez-Reinoso F, Rouquerol J, et al. Physisorption of gases, with special reference to the evaluation of surface area and pore size distribution (IUPAC Technical Report). Pure Appl Chem 2015;87:1051–69. https://doi.org/10.1515/pac-2014-1117.
[208] Yan D, Chen S, Zeng Q, Xu S, Li H. Correlating the elastic properties of metakaolin-based geopolymer with its composition. JMADE 2016. https://doi.org/10.1016/j.matdes.2016.01.107.
[209] Yang T, Zhu H, Zhang Z. Influence of fly ash on the pore structure and shrinkage characteristics of metakaolin-based geopolymer pastes and mortars. Constr Build Mater 2017;153:284–93. https://doi.org/10.1016/j.conbuildmat.2017.05.067.
[210] Zhang Z, Wang H, Zhu Y, Reid A, Provis JL, Bullen F. Using fly ash to partially substitute metakaolin in geopolymer synthesis. Appl Clay Sci 2014:88–9. https://doi.org/10.1016/j.clay.2013.12.025. 194–201.
[211] Lolli F, Manzano H, Provis JL, Bignozzi MC, Masoero E. Atomistic simulations of geopolymer models : the impact of disorder on structure and mechanics. ACS Appl Mater Interfac 2018. https://doi.org/10.1021/acsami.8b03873.
[212] Yang K, White CE. Multiscale pore structure determination of cement paste via simulation and experiment: the case of alkali-activated metakaolin. Cement Concr Res 2020;137:106212. https://doi.org/10.1016/j.cemconres.2020.106212.
[213] Tan TH, Mo KH, Ling TC, Lai SH. Current development of geopolymer as alternative adsorbent for heavy metal removal. Environ Technol Innovat 2020;18:100684. https://doi.org/10.1016/j.eti.2020.100684.
[214] Sultana M, Rownok MH, Sabrin M, Rahaman MH, Alam SMN. A review on experimental chemically modified activated carbon to enhance dye and heavy metals adsorption. Clean Eng Technol 2022;6:100382. https://doi.org/10.1016/j.clet.2021.100382.
[215] Abegunde SM, Idowu KS, Adejuwon OM, Adeyemi-Adejolu T. A review on the influence of chemical modification on the performance of adsorbents. Resour Environ Sustain 2020;1:100001. https://doi.org/10.1016/j.resenv.2020.100001.
[216] Luo Y, Li SH, Klima KM, Brouwers HJH, Yu Q. Degradation mechanism of hybrid fly ash/slag based geopolymers exposed to elevated temperatures. Cement and Concrete Research 2022;151. https://doi.org/10.1016/j.cemconres.2021.106649.
[217] Liu X, Jiang J, Zhang H, Li M, Wu Y, Guo L, et al. Thermal stability and microstructure of metakaolin-based geopolymer blended with rice husk ash. Appl Clay Sci 2020;196:105769. https://doi.org/10.1016/j.clay.2020.105769.
[218] Lemougna PN, Adediran A, Yliniemi J, Ismailov A, Levanen E, Tanskanen P, et al. Thermal stability of one-part metakaolin geopolymer composites containing high volume of spodumene tailings and glass wool. Cem Concr Compos 2020;114:103792. https://doi.org/10.1016/j.cemconcomp.2020.103792.
[219] Pachana PK, Rattanasak U, Nuithitikul K, Jitsangiam P, Chindaprasirt P. Sustainable utilization of water treatment residue as a porous geopolymer for iron and manganese removals from groundwater. J Environ Manag 2022;302:114036. https://doi.org/10.1016/j.jenvman.2021.114036.
[220] Lahoti M, Wijaya SF, Tan KH, Yang EH. Tailoring sodium-based fly ash geopolymers with variegated thermal

performance. Cem Concr Compos 2020;107:103507. https://doi.org/10.1016/j.cemconcomp.2019.103507.
[221] Attia AA, Rashwan WE, Khedr SA. Capacity of activated carbon in the removal of acid dyes subsequent to its thermal treatment. Dyes Pigment 2006;69:128–36. https://doi.org/10.1016/j.dyepig.2004.07.009.
[222] Xiang W, Zhang X, Chen K, Fang J, He F, Hu X, et al. Enhanced adsorption performance and governing mechanisms of ball-milled biochar for the removal of volatile organic compounds (VOCs). Chem Eng J 2020;385:123842. https://doi.org/10.1016/j.cej.2019.123842.
[223] Li Y, Zimmerman AR, He F, Chen J, Han L, Chen H, et al. Solvent-free synthesis of magnetic biochar and activated carbon through ball-mill extrusion with Fe3O4 nanoparticles for enhancing adsorption of methylene blue. Sci Total Environ 2020;722:137972. https://doi.org/10.1016/j.scitotenv.2020.137972.
[224] Du H, Xi C, Tang B, Chen W, Deng W, Cao S, et al. Performance and mechanisms of NaOH and ball-milling co-modified biochar for enhanced the removal of Cd2+ in synthetic water: a combined experimental and DFT study. Arab J Chem 2022;15:103817. https://doi.org/10.1016/j.arabjc.2022.103817.
[225] Arokiasamy P, Al Bakri Abdullah MM, Abd Rahim SZ, Luhar S, Sandu AV, Jamil NH, et al. Synthesis methods of hydroxyapatite from natural sources: a review. Ceram Int 2022. https://doi.org/10.1016/j.ceramint.2022.03.064.
[226] Baláž P, Achimovicová M, Baláž M, Billik P, Zara CZ, Criado JM, et al. Hallmarks of mechanochemistry: from nanoparticles to technology. Chem Soc Rev 2013;42:7571–637. https://doi.org/10.1039/c3cs35468g.
[227] Wang K, Liu X, Tang J, Wang L, Sun H. Ball milled Fe0@FeS hybrids coupled with peroxydisulfate for Cr(VI) and phenol removal: novel surface reduction and activation mechanisms. Sci Total Environ 2020;739:139748. https://doi.org/10.1016/j.scitotenv.2020.139748.
[228] Li R, Zhang Y, Deng H, Zhang Z, Wang JJ, Shaheen SM, et al. Removing tetracycline and Hg(II) with ball-milled magnetic nanobiochar and its potential on polluted irrigation water reclamation. J Hazard Mater 2020;384. https://doi.org/10.1016/j.jhazmat.2019.121095.
[229] Lyu H, Gao B, He F, Ding C, Tang J, Crittenden JC. Ball-milled carbon nanomaterials for energy and environmental applications. ACS Sustainable Chem Eng 2017;5:9568–85. https://doi.org/10.1021/acssuschemeng.7b02170.
[230] Gorrasi G, Sorrentino A. Mechanical milling as a technology to produce structural and functional bio-nanocomposites. Green Chem 2015;17:2610–25. https://doi.org/10.1039/c5gc00029g.
[231] Ge Y, Cui X, Kong Y, Li Z, He Y, Zhou Q. Porous geopolymeric spheres for removal of Cu(II) from aqueous solution: synthesis and evaluation. J Hazard Mater 2015;283:244–51. https://doi.org/10.1016/j.jhazmat.2014.09.038.
[232] Hu H, Li X, Huang P, Zhang Q, Yuan W. Ef fi cient removal of copper from wastewater by using mechanically activated calcium carbonate. J Environ Manag 2017;203:1–7. https://doi.org/10.1016/j.jenvman.2017.07.066.

Mohd Mustafa Al Bakri Abdullah, currently he is Professor at Universiti Malaysia Perlis (UniMAP); Area of expertise are concrete processing and testing, geopolymer concrete, green concrete, composite, ceramic, and polymeric concrete. Between 2005 and April 2021, he was appointed several positions such as College Principal, Deputy Dean (Students Affair), Dean (Centre of Diploma Studies, Director (Research Management Centre) and the highest position is an Acting Deputy Vice Chancellor (Research & Innovation) starting 2020 until May 2021. He was awarded Top Research Malaysia (TRMS) in 2013 and received several awards from international and national organizations based on his geopolymer research. Now he is one of the specialists in the geopolymer field and established **Center of Excellence Geopolymer & Green Technology (CEGeoGTech)**, UniMAP the only geopolymer center in ASEAN. This center is number one in ther world for geopolymers based on publications. He also has research funding and collaboration with King AbdulAziz City Science & Technoloy (KACST) Saudi Arabia, European Commission, University of Plymouth UK, Liverpool John Moores University UK and also with few more universities from Greece, Poland, Romania and Indonesia. His achievements include more than 650 journal publications based on Scopus Database (with 37 h-index), and more than 35 books and 40 patents of his research product. He has appointed as Research Advisor to State University of Makassar Indonesia and Associate Researcher in Technical University of Iasi (TUIASI) & Technical University of Cluj-Napoca, Romania and University of Chemical Technology and Metallurgy (UCTM), Bulgaria